Astronomy & Astrophysics manuscript no. nacolp-survey-v6rev-astroph
May 8, 2014

The VLT/NaCo large program to probe the occurrence of exoplanets and brown dwarfs at wide orbits*

II- Survey description, results and performances

G. Chauvin[1], A. Vigan[2], M. Bonnefoy[3], S. Desidera[4], M. Bonavita[4], D. Mesa[4], A. Boccaletti[5], E. Buenzli[3], J. Carson[6,3], P. Delorme[1], J. Hagelberg[7], G. Montagnier[2], C. Mordasini[3], S.P. Quanz[8], D. Segransan[7], C. Thalmann[8], J.-L. Beuzit[1], B. Biller[3], E. Covino[9], M. Feldt[3], J. Girard[10], R. Gratton[4], T. Henning[3], M. Kasper[11], A.-M. Lagrange[1], S. Messina[12], M. Meyer[8], D. Mouillet[1], C. Moutou[2], M. Reggianni[8], J.E. Schlieder[3], and A. Zurlo[2]

[1] UJF-Grenoble1/CNRS-INSU, Institut de Planétologie et d'Astrophysique de Grenoble UMR 5274, Grenoble, F-38041, France
[2] Aix Marseille Université, CNRS, LAM (Laboratoire d'Astrophysique de Marseille) UMR 7326, 13388 Marseille, France
[3] Max Planck Institute for Astronomy, Königstuhl 17, D-69117 Heidelberg, Germany
[4] INAF - Osservatorio Astronomico di Padova, Vicolo dell Osservatorio 5, 35122, Padova, Italy
[5] LESIA, Observatoire de Paris Meudon, 5 pl. J. Janssen, 92195 Meudon, France
[6] Department of Physics & Astronomy, College of Charleston, 58 Coming Street, Charleston, SC 29424, USA
[7] Geneva Observatory, University of Geneva, Chemin des Mailettes 51, 1290 Versoix, Switzerland
[8] Institute for Astronomy, ETH Zurich, Wolfgang-Pauli-Strasse 27, 8093 Zurich, Switzerland
[9] INAF Osservatorio Astronomico di Capodimonte Via Moiarello 16 80131 Napoli Italy
[10] European Southern Observatory, Casilla 19001, Santiago 19, Chile
[11] European Southern Observatory, Karl Schwarzschild St, 2, D-85748 Garching, Germany
[12] INAF - Catania Astrophysical Observatory, via S. So a 78 I-95123 Catania, Italy

Preprint online version: May 8, 2014

ABSTRACT

Context. Young, nearby stars are ideal targets for direct imaging searches for giant planets and brown dwarf companions. After the first imaged planets discoveries, vast efforts have been devoted to the statistical analysis of the occurence and orbital distributions of giant planets and brown dwarf companions at wide ($\geq 5-6$ AU) orbits.

Aims. In anticipation of the VLT/SPHERE planet imager guaranteed time programs, we have conducted a preparatory survey of 86 stars between 2009 and 2013 in order to identify new faint comoving companions to ultimately carry out a comprehensive analysis of the occurence of giant planets and brown dwarf companions at wide ($10-2000$ AU) orbits around young, solar-type stars.

Methods. We used NaCo at VLT to explore the occurrence rate of giant planets and brown dwarfs between typically 0.1 and 8″. Diffraction-limited observations in H-band combined with angular differential imaging enabled us to reach primary star-companion brightness ratios as small as 10^{-6} at 1.5″. Repeated observations at several epochs enabled us to discriminate comoving companions from background objects.

Results. 12 systems were resolved as new binaries, including the discovery of a new white dwarf companion to the star HD 8049. Around 34 stars, at least one companion candidate was detected in the observed field of view. More than 400 faint sources were detected, 90% of them in 4 crowded fields. With the exception of HD 8049 B, we did not identify any new comoving companions. The survey also led to spatially resolved images of the thin debris disk around HD 61005 that have been published earlier. Finally, considering the survey detection limits, we derive a preliminary upper limit on the frequency of giant planets for semi-major axes of [10,2000] AU: typically less than 15% between 100 and 500 AU, and less than 10% between 50 and 500 AU for exoplanets more massive than 5 M_{Jup} and 10 M_{Jup} respectively, considering a uniform input distribution and with a confidence level of 95%.

Conclusions. The results from this survey are in agreement with earlier programs emphasizing that massive, gas giant companions on wide orbits around solar-type stars are rare. They will be part of a broader analysis of a total of ~ 210 young, solar-type stars to bring further statistical constraints for theoretical models of planetary formation and evolution.

Key words. Instrumentation: adaptive optics, high angular resolution – Methods: observational, statistical – Techniques: image processing – Surveys – Stars: close binaries, planetary systems, brown dwarfs – Infrared: stars, planetary systems

1. Introduction

Our understanding of the origin and evolution of extrasolar planets (EPs) has drastically transformed in the last decade. Current theories favor the formation of planets within a protoplanetary disk by accretion of solids, building up a 10 to 15 $M_\oplus$ core followed by rapid agglomeration of gas (Pollack et al. 1996; Alibert et al. 2004), or by gravitational instability of the gas (Boss 1997; Stamatellos & Withworth 2008; Vorobyov 2013). Whereas physical conditions and timescales favor core accretion in the inner disk ($\leq$ 10 AU), gravitational instability could be the main mechanism to form massive gaseous giants at wider separations ($\geq$ 10 AU) in the earliest phase of the disk's lifetime (Boley 2009). The planets could either migrate inward, toward or outward, from the star by disk-planet interactions (Kley & Nelson 2012 and reference therein) or during planet-planet interactions (Naoz et al. 2011; Dawson & Murray-Clay 2013), which will alter the original semi-major axis distribution. A wide range of potential planet masses, sizes, locations and compositions results from this flurry of formation and evolution possibilities. A major goal for exoplanetary science of the next decade is a better understanding of these mechanisms. In this context, the role of observations is crucial to provide constraints that will help to model the diversity of exoplanetary properties. The main observables are the occurrence of EPs, the physical and orbital characteristics (composition, mass, radius, luminosity, distribution of mass, period and eccentricity), but also the properties of the planetary hosts (mass, age, metallicity, lithium abundance or multiplicity).

Brown dwarfs (BDs) were originally proposed as a distinguishable class of astrophysical objects, with intermediate masses between stars and planets. Recent large infrared surveys and high contrast observations have unambiguously revealed the existence of planetary mass objects, isolated in the field (Zapatero-Osorio et al. 2000; Liu et al. 2013; Joergens et al. 2013) or wide companions to stars (Chauvin et al. 2005a). Their existence confirms that the formation mechanisms proposed to form stars (gravo-turbulent fragmentation, disk fragmentation, accretion-ejection or photoerosion; see Whitworth et al. 2007, Luhman 2012 for reviews) can actually form objects down to the planetary mass regime. The details of contraction and subsequent evolution of the cores remain critical and are still under considerable debate. Episodic accretion processes can affect their physical properties (Baraffe et al. 2009). It is now undeniable that the stellar and planetary formation mechanisms overlap in the substellar regime. They can both lead to the formation of planetary mass objects, including companions to stars and BDs. Fossil traces of the formation processes should be revealed by different physical features (presence of core, composition of the atmosphere, system architecture...). Distinct statistical properties such as the occurrence, the mass, separation and eccentricity distributions, should help to identify the dominant mechanism to form substellar companions.

The main statistical constraints on exoplanets originally came from the radial velocity (RV) technique. More than 800 EPs have been now confirmed, featuring a broad range of physical (mass) and orbital (P, e) characteristics around different stellar hosts (Howard et al. 2010; Mayor et al. 2011; Wright et al. 2012; Bonfils et al. 2013). The strong bimodal aspect of the secondary-mass distribution to solar-type primaries has generally been considered the most obvious evidence of different formation mechanisms for stellar and planetary systems. The period distribution of giant exoplanets is basically made of two main features: a peak around 3 days plus an increasing frequency as a function of period (Udry & Santos 2007). The observed pile up of planets with periods around 3 days is believed to be the result of migration and final stopping mechanism. The rise of the number of planets with increasing distance from the parent star reaches up to a separation corresponding to the duration limit of most of the longest surveys (5-6 AU). This extrapolation hints that a large population of yet undetected Jupiter-mass planets may exist beyond 5 AU, suggesting an ideal niche for the direct-imaging surveys. More recently, a plethora of transiting planetary candidates have been revealed by *Kepler* (more than 2300 candidates known today, Batalha et al. 2013), probably corroborating how abundant telluric planets are and in agreement with Doppler surveys in terms of occurrence at less than 0.25 AU (Howard et al. 2012).

Despite the success of the RV and transit techniques, the time spans explored limit the studies to the close ($\leq 5-6$ AU) EPs. Within the coming years, direct imaging represents the only viable technique for probing the existence of EPs and BD companions at large ($\geq 5-6$ AU) separations. This technique is also unique for the characterization of planetary atmospheres that are not strongly irradiated by the planetary host (Janson et al. 2010; Bowler et al. 2010; Barman et al. 2011a, 2011b; Bonnefoy et al. 2010, 2013a, 2013b, 2013c; Konopacky et al. 2013). Young ($\leq$ 500 Myr), nearby stars are very favourable targets for the direct detection of the lowest mass companions. Since the discovery of the TW Hydrae association (TWA) by Kastner et al. (1997) and Hoff et al. (1998), more than 300 young, nearby stars were identified. They are gathered in several groups (TWA, β Pictoris, Tucana-Horologium, η Cha, AB Dor, Columba, Carinae), sharing common kinematics, photometric and spectroscopic properties (see Zuckerman & Song 2004; Torres et al. 2008). With typical contrast of $10-15$ magnitudes for separations beyond $1.0-2.0''$ ($50-100$ AU for a star at 50 pc), planetary mass companions down to $1-2$ Jupiter masses are potentially detectable by current very deep imaging surveys. The first planetary mass companions were detected at large distances ($\geq$ 100 AU) and/or with small mass ratio with their primaries, indicating a probable star-like or gravitational disk instability formation mechanism (Chauvin et al. 2005b; Lafrenière et al. 2008).

The breakthrough discoveries of closer and/or lighter planetary mass companions like Fomalhaut b (<1 M_{Jup} at 177 AU; Kalas et al. 2008, 2013), HR 8799 bcde (10, 10, 10 and 7 M_{Jup} at resp. 14, 24, 38 and 68 AU; Marois et al. 2008, 2010), β Pictoris b (8 M_{Jup} at 8 AU; Lagrange et al. 2009) or more recently κ And b (14^{+25}_{-2} M_{Jup} at 55 AU; Carson et al. 2013; Bonnefoy et al. 2013c), HD 95086 b ($4-5$ M_{Jup} at 56 AU; Rameau et al. 2013a, 2013b) and GJ 504 b ($4^{+4.5}_{-1}$ M_{Jup} at 43.5 AU; Kuzuhara et al. 2013) indicate that we are just initiating the characterization of the outer part of planetary systems between typically $5-100$ AU. Vast efforts are now devoted to systematic

⋆ Based on observations collected at the European Southern Observatory, Chile (ESO Large Program 184.C-0157 and Open Time 089.C-0137A and 090.C-0252A)

Table 1. Deep imaging surveys of young (< 100 Myr) and intermediate-old to old (0.1 − 5 Gyr), nearby (< 100 pc) stars dedicated to the search for planetary mass companions. We have indicated the telescope and the instrument, the imaging mode (Cor-I: coronagraphic imaging; Sat-I; saturated imaging; I: imaging; SDI: simultaneous differential imaging; ADI: angular differential imaging; ASDI: angular and spectral differential imaging), the filters, the field of view (FoV), the number of stars observed (#), their spectral types (SpT) and ages (Age).

Reference	Telescope	Instr.	Mode	Filter	FoV (″×″)	#	SpT	Age (Myr)
Chauvin et al. 2003	ESO3.6m	ADONIS	Cor-I	H, K	13 × 13	29	GKM	$\lesssim 50$
Neuhäuser et al. 2003	NTT	Sharp	Sat-I	K	11 × 11	23	AFGKM	$\lesssim 50$
	NTT	Sofi	Sat-I	H	13 × 13	10	AFGKM	$\lesssim 50$
Lowrance et al. 2005	HST	NICMOS	Cor-I	H	19 × 19	45	AFGKM	10 − 600
Masciadri et al. 2005	VLT	NaCo	Sat-I	H, K	14 × 14	28	KM	$\lesssim 200$
Biller et al. 2007	VLT	NaCo	SDI	H	5 × 5	45	GKM	$\lesssim 300$
	MMT		SDI	H	5 × 5	-	-	-
Kasper et al. 2007	VLT	NaCo	Sat-I	L'	28 × 28	22	GKM	$\lesssim 50$
Lafrenière et al. 2007	Gemini-N	NIRI	ADI	H	22 × 22	85		10-5000
Apai et al. 2008[a]	VLT	NaCo	SDI	H	3 × 3	8	FG	12-500
Chauvin et al. 2010	VLT	NaCo	Cor-I	H, K	28 × 28	88	BAFGKM	$\lesssim 100$
Heinze et al. 2010ab	MMT	Clio	ADI	L', M	15.5 × 12.4	54	FGK	100-5000
Janson et al. 2011	Gemini-N	NIRI	ADI	H, K	22 × 22	15	BA	20-700
Vigan et al. 2012	Gemini-N	NIRI	ADI	H, K	22 × 22	42	AF	10-400
	VLT	NaCo	ADI	H, K	14 × 14	-	-	-
Delorme et al. 2012	VLT	NaCo	ADI	L'	28 × 28	16	M	$\lesssim 200$
Rameau et al. 2013c	VLT	NaCo	ADI	L'	28 × 28	59	AF	$\lesssim 200$
Yamamoto et al. 2013	Subaru	HiCIAO	ADI	H, K	20 × 20	20	FG	125 ± 8
Biller et al. 2013	Gemini-S	NICI	Cor-ASDI	H	18 × 18	80	BAFGKM	$\lesssim 200$
Brandt et al. 2013[b]	Subaru	HiCIAO	ADI	H	20 × 20	63	AFGKM	$\lesssim 500$
Nielsen et al. 2013	Gemini-S	NICI	Cor-ASDI	H	18 × 18	70	BA	50-500
Wahhaj et al. 2013[a]	Gemini-S	NICI	Cor-ASDI	H	18 × 18	57	AFGKM	∼ 100
Janson et al. 2013[a]	Subaru	HiCIAO	ADI	H	20 × 20	50	AFGKM	$\lesssim 1000$

- ([a]): surveys dedicated to planets around debris disk stars.
- ([b]): paper submitted.

searches of EPs in direct imaging with an increasing number of large scale surveys (see Table 1; nine new surveys published between 2012 and 2013). The number of targets surveyed and the detection performances will increase with the new generation of planet finders LMIRCam at LBT (Skrustkie et al. 2010), MagAO (Close et al. 2012), ScExAO at Subaru (Guyon et al. 2010), SPHERE at VLT (Beuzit et al. 2008), GPI at Gemini (Macintosh et al. 2008) with the goal to provide better statistics on larger samples and a greater number of giants planets to be characterized. It should enable to test alternative mechanisms to the standard planetary formation theories of core accretion and gravitation instability such as pebble accretion (Lambrechts & Johansen 2012; Morbidelli & Nesvorny 2012) or tidal downsizing (Boley et al. 2010; Nayakshin 2010; Forgan & Rice 2013) that are currently proposed to explain the existence of a population of giant planets at wide orbits. In the context of the VLT/SPHERE scientific preparation, we have conducted a large observing program (ESO: 184.C-0157) of 86 stars with NaCo (hereafter the NaCo-LP). Combined with stars already observed in direct imaging, it represents a total of more than ∼ 210 stars to study the occurrence rate of giant planets and brown dwarf companions at wide (10 − 2000 AU) orbits. This complete analysis is detailed in series of four papers: a description of the complete sample (Desidera et al. 2013, submitted), the NaCo-LP survey (this paper) and the statistical analysis of the giant planet population (Vigan et al. 2014, in prep) and of the brown dwarf companion population (Reggianni et al. 2014, in prep). We therefore report here the results of the NaCo-LP carried out between 2009 and 2013. In Section 2, we describe the target sample selection. In Section 3, we detail the observing setup. In Section 4, the data reduction strategy and analysis are reported with the results in Section 5. Finally, a preliminary statistical analysis of the observed sample is presented in Section 6 and our main conclusions in Section 7.

2. Target Properties

Based on a complete compilation of young, nearby stars, recently identified in young co-moving groups and from systematic spectroscopic surveys, we have selected a sample of stars according to: their declination ($\delta \leq 25^o$), their age ($\lesssim$ 200 Myr), their distance ($d \lesssim 100$ pc), their R-band brightness ($R \leq 9.5$). In addition, none of these stars had been observed in a high-contrast imaging survey before. Great care has been taken in the age selection criteria based on different youth diagnostics (isochrones, lithium abundance, Hα emission, X-ray activity, stellar rotation, chromospheric activity and kinematics). Close visual (0.1−6.0″) and spectroscopic binaries were rejected as they degrade the VLT/NaCo detection performances and bias the astrophysical interpretation. Among this sample, 86 stars were finally observed during the large program. The main target properties (spectral type, distance, age, H-band magnitude, galactic latitude, proper motion) are reported in Tables 2 and 3. They are also shown in Fig. 1 together with the prop-

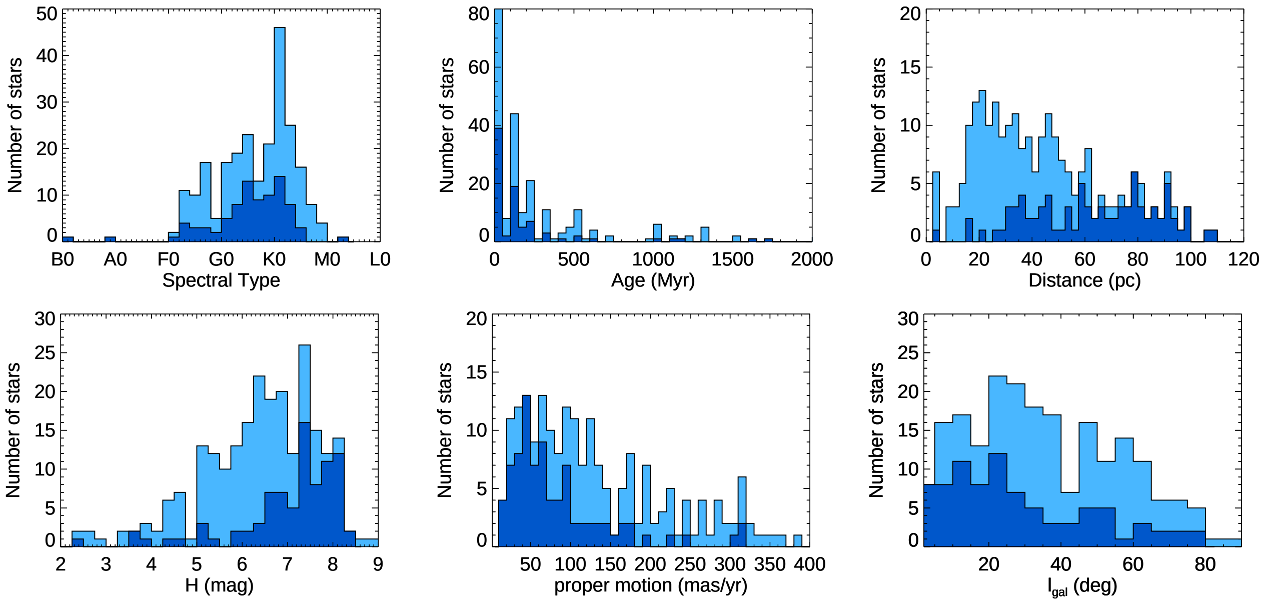

Fig. 1. Histrograms summarizing the main properties of NaCo-LP observed sample (*dark blue*) and of the final NaCo-LP statistical sample of ∼210 stars (*light blue*) used by Vigan et al. (2014, in prep) and Reggianni et al. (2014, in prep): spectral type, age, distance, H-band magnitude, proper motion amplitude and galactic latitude.

Table 4. Observing campaigns with the ESO-program number, the observing mode (LP for Large-Program; OT for Open-Time; Vis for Visitor run and Ser for Service run), the starting night and the number of nights, the observing loss (technical and weather) and the number of observing sequences including single and multiple visits per target.

ESO Program	Mode	St. Night (UT-date)	Night (Nb)	Loss (%)	Visit (Nb)
184.C-0157A	LP-Vis	2009-11-21	3	20	23
184.C-0157E	LP-Vis	2010-02-16	3	0	27
184.C-0157B	LP-Vis	2010-06-14	2.5	70	11
184.C-0157F	LP-Vis	2010-07-29	2	33	18
184.C-0157C	LP-Ser	-	1.5	0	15
184.C-0157D	LP-Ser	-	3.3	0	33
089.C-0137A	OT-Ser	-	0.7	0	6
090.C-0252A	OT-Ser	-	0.5	0	4
Total	-	-	16.5		137

erties of the complete statistical sample used by Vigan et al. (2014, in prep) and Reggianni et al. (2014, in prep). A complete characterization of the NaCo-LP observed sample and the archive sample, particularly the age and distance determination, is detailed by Desidera et al. (2013, submitted). As can be seen from Fig. 1, the core of the NaCo-LP observed sample is mainly composed of young (10–200 Myr), nearby solar-type FGK stars.

3. Observations: Telescope and instrument

We used the NaCo high contrast Adaptive Optics (AO) imager of the VLT-UT4. NaCo is equipped with the NAOS AO system (Rousset et al. 2002), and the near infrared imaging camera CONICA (Lenzen et al. 2002). The observations were obtained during various observing runs spread between end 2009 and 2013 in visitor and service (queue-observing) modes. The summary of the observing runs is reported in Table 4. The NaCo-LP represents a total of 16.5 observing nights, 10.5 nights obtained in visitor mode and 6 nights in service.

To achieve high contrasts, we used the angular differential imaging (ADI) on pupil-stabilized mode of NaCo. A classical Lyot-coronagraph with a diameter of 0.7″ was used during the first visitor run but then replaced by saturated imaging as the NaCo PSF was unexpectedly drifting with time owing to a technical problem with the instrument. For accurate astrometry, a single observing set-up was used, corresponding to the combined use of the H-band filter with the S13 camera (13.25 mas/pix). The time of the observations were chosen to maximize the field rotation. Typical exposure times of 1–10s were used to saturate the PSF core by a factor 100 (a few pixels in radius) to improve the dynamic range of our images. The NaCo detector cube mode was in addition used to register each individual frames to optimize the final image selection in post-processing. The typical observing sequence was composed of a total of 10–15 cubes of 10–120 frames, i.e a total integration time of 35–40 min for an observing sequence of 1–1.5 hrs on target. The parallactic angles variations are reported in Fig. 2 together with the airmass, coherent energy and coherent time measured by NaCo and the seeing measured by the DIMM seeing monitor at VLT. Non-saturated PSFs were acquired in ADI using a neutral density filter at the beginning of each observing sequence to monitor the image quality. They also served for the calibration of the relative photometric and astrometric measurements.

4. Data reduction and analysis

4.1. Cosmetics and data processing

Three independent pipelines were used to reduce and analyse the ADI data in order to optimize the PSF-subtraction and the detection performances and to check the consistency of the results in terms of astrometry and photometry. These pipelines are described for: the LAM-ADI pipeline by

Table 2. NaCo-LP target sample and properties. In addition to the target name, H-band magnitude, spectral type, distance and age, we have reported the multiplicity status with a flag (Bin for visual binaries with the indication that they are new or known; SB for spectroscopic binaries; RV var for radial velocity variable), the observing mode (nonsat for non-saturated or sat for saturated, ADI for angular differential imaging and the filter) and the presence of companion candidates (ccs).

Name-1	Name-2	H (mag)	SpT	d (pc)	Age (Myr)	Binarity	Mode	Comments
TYC 5839-0596-1	BD-16-20	6.6	K0IVe	43.5	150.	SB2	sat, ADI, H	
TYC 0603-0461-1	BD+07-85	7.4	K4Ve	58.2	100.	Bin (new)	sat, ADI, H	
HIP3924	HD4944	6.7	F7V	53.2	500.	SB2	sat, ADI, H	
HIP6177	HD8049	6.7	K2V	33.6	3000.		sat, ADI, H	cc
HIP8038	HD10611B	7.2	K5Ve	29.3	150.	Bin (new)	nonsat, ADI, H	
HIP10602	HD14228	4.0	B0V	47.1	30.		sat, ADI, H	
HIP11360	HD15115	5.9	F2	45.2	30.		sat, ADI, H	
TYC 8484-1507-1	CD-53-535	6.6	G8V	60.5	100.	Bin (known)	nonsat, ADI, H	
HIP12394	HD16978	4.4	B9III	46.6	30.		sat, ADI, H	
HIP13008	HD17438	5.5	F2V	39.6	1000.		sat, ADI, H	cc
HIP14684	IS-Eri	6.8	G0	37.4	100.		sat, ADI, H	cc
TYC 8060-1673-1	CD-46-1064	7.2	K3V	40.4	30.		sat, ADI, H	
HIP19775	HD26980	7.7	G3V	80.5	30.		sat, ADI, H	
HIP23316	HD32372	7.9	G5V	76.3	30.		sat, ADI, H	
HD32981	BD-16-1042	7.8	F8V	86.7	100.		sat, ADI, H	
BD-09-1108	xxxx	8.2	G5	93.6	30.		sat, ADI, H	
HIP25434	HD274197	7.9	G0	79.1	20.		sat, ADI, H	ccs
TYC 9162-0698-1	HD269620	8.2	G6V	77.7	30.		sat, ADI, H	ccs
TYC 5346-132-1	BD-08-1195	8.1	G7	81.2	30.		sat, ADI, H	ccs
HIP30261	HD44748	7.6	G6V	61.8	100.		sat, ADI, H	
TYC 7617-0549-1	CD-40-2458	8.2	K0V	77.8	30.		sat, ADI, H	cc
TYC 9181-0466-1	HD47875	7.4	G4V	77.7	30.	Bin (new)	nonsat, ADI, H	
HIP32235	HD49855	7.4	G6V	58.2	30.		sat, ADI, H	cc
HIP35564	HD57852	5.1	F2	31.7	200.	RV var	sat, ADI, H	ccs
TYC 8128-1946-1	CD-48-2972	8.1	G8V	89.7	45.		sat, ADI, H	ccs
HIP36414	HD59704	6.5	F7V	52.5	200.	SB, RV var	sat, ADI, H	ccs
HIP36948	HD61005	6.6	G5V	35.3	45.		sat, ADI, H	ccs
HIP37563	HD62850	5.9	G3V	32.8	200.		sat, ADI, H	
HIP37923	HD63608	6.5	K0V	36.8	200.		sat, ADI, H	ccs
TYC 8927-3620-1	HD77307	7.7	G8IV	81.8	20.	Bin (new)	sat, ADI, H	
HIP46634	BD+11-2052B	6.8	G5	42.3	300.		sat, ADI, H	
HIP47646	HD84199	6.9	F5V	73.6	1150.		sat, ADI, H	
TWA-21	HD298936	7.3	K3Ve	54.8	17.		sat, ADI, H	ccs
TYC 7188-0575-1	CD-31-8201	7.4	K0Ve	43.2	150.	SB2	sat, ADI, H	ccs
TYC 6069-1214-1	BD-19-3018	8.0	K0V	67.8	70.		sat, ADI, H	
TYC 7722-0207-1	HD296790	7.8	K0V	65.8	100.		sat, ADI, H	ccs
TYC 7743-1091-1	HD99409	5.2	G6III	200.0	1700.		sat, ADI, H	
HIP58240	HD103742	6.2	G3V	31.8	200.		sat, ADI, H	cc
TYC 9231-1566-1	HD105923	7.3	G8V	96.0	10.	Bin (new)	nonsat, ADI, H	
TYC 8979-1683-1	CD-62-657	7.5	G7V	75.6	17.		sat, ADI, H	ccs
TYC 8989-0583-1	HD112245	7.4	K0Ve	65.4	17.	Bin (new)	sat, ADI, H	
TYC 9245-0617-1	CD-69-1055	7.7	K0Ve	93.0	10.		sat, ADI, H	ccs
HIP63862	HD113553	6.8	G5V	49.0	150.		sat, ADI, H	ccs
TYC 7796-2110-1	CD-41-7947	8.3	K2IVe	92.1	17.		sat, ADI, H	ccs
TYC 9010-1272-1	HD124831	7.8	G3V	86.5	30.	Bin (new)	nonsat, ADI, H	
HIP70351	HD125485	7.6	G7V	91.7	110.		sat, ADI, H	ccs
HIP71908	GJ-560A	2.5	F1V	16.6	1110.		sat, ADI, H	cc
HIP71933	HD129181	7.2	F8V	83.9	16.		sat, ADI, H	ccs
HIP72399	HD130260A	7.5	K3Ve	46.1	500.	SB1, RV var	sat, ADI, H	
TYC 7835-2569-1	HD137059	7.1	G3V	70.2	120.	SB2 + Bin (known)	sat, ADI, H	
HIP76829	HD139664	3.7	F5IV	17.4	200.		sat, ADI, H	ccs
TYC 6781-0415-1	CD-24-12231	7.4	G9IVe	106.0	11.		sat, ADI, H	
TYC 6786-0811-1	CD-27-10549	7.5	K0IV	78.6	60.	Bin (known)	nonsat, ADI, H	
HIP78747	HD143928	5.1	F3V	37.9	1600.		sat, ADI, H	ccs
TYC 6209-0769-1	BD-19-4341	7.4	K0IV	43.9	120.		sat, ADI, H	cc
HIP79958	HD146464	6.7	K3Ve	27.2	130.		sat, ADI, H	ccs
HIP80290	HD147491	8.0	G2IV	83.3	30.	Bin (new)	sat, ADI, H	ccs
HIP80758	HD148440	8.0	G9Ve	98.2	20.		sat, ADI, H	ccs

Table 3. NaCo-LP target sample and properties (Table 2-cont).

Name-1	Name-2	H (mag)	SpT	d (pc)	Age (Myr)	Binarity	Mode	Comments
TYC 6818-1336-1	HD153439	7.8	G0IV	89.5	30.		sat, ADI, H	ccs
TYC 6815-0084-1	CD-25-11942	7.7	K0IV	92.0	11.		sat, ADI, H	ccs
TYC 6815-0874-1	CD-25-11922	10.1	G2IV	109.0	20	SB2?	sat, ADI, H	ccs
TYC 7362-0724-1	HD156097	7.8	G5V	90.0	20.		sat, ADI, H	ccs
TYC 8728-2262-1	CD-54-7336	7.5	K1V	70.4	12.		sat, ADI, H	ccs
HIP86672	HD160682	7.4	G5V	78.0	30.		sat, ADI, H	ccs
HIP89829	HD168210	7.2	G5V	72.6	16.		sat, ADI, H	ccs
HIP93375	HD176367	7.3	G1V	58.8	100.		sat, ADI, H	ccs
HIP94235	HD178085	7.0	G1V	61.3	100.	Bin (new)	nonsat, ADI, H	
TYC 6893-1391-1	CD-25-14224	7.8	K2V	55.1	160.		sat, ADI, H	ccs
TYC 5206-0915-1	BD-07-5533	8.2	K1IV	76.4	300.		sat, ADI, H	
TYC 5736-0649-1	BD-14-5534	8.0	G6V	86.4	30.		sat, ADI, H	ccs
HD189285	BD-04-4987	8.0	G5	77.8	100.		sat, ADI, H	cc
HIP98470	HD189245	4.6	F7V	21.2	100.		sat, ADI, H	
TYC 5164-567-1	BD-03-4778	8.0		63.3	100.		sat, ADI, H	ccs
HIP99273	HD191089	6.1	F5V	52.2	16.		sat, ADI, H	
HD199058	BD+08-4561	7.0	G5	66.2	100.	Bin (new)	nonsat, ADI, H	
HIP105384	HD203019	6.4	K5V	35.0	400.		sat, ADI, H	cc
HIP105612	HD202732	6.3	G5V	32.8	600.		sat, ADI, H	
HIP107684	HD207278	8.1	G7V	90.2	100.	Bin (new)	nonsat, ADI, H	
HIP108422	HD208233	6.9	G9IV	58.0	30.	Bin (known)	nonsat, ADI, H	
TYC 8004-0083-1	CD-40-14901	7.9	G5V	74.9	100.		sat, ADI, H	
HIP114046	HD217897	3.6	M2V	3.3	8000.		sat, ADI, H	
TYC 9338-2016-1	HD220054	8.3	G8V	99.6	30.		sat, ADI, H	
TYC 9529-0340-1	CD-86-147	7.6	G8IV	68.8	30.		sat, ADI, H	
TYC 9339-2158-1	CD-69-2101	6.8	K3V	30.6	300.		sat, ADI, H	
TYC 6406-0180-1	HD221545	7.7	K0V	58.0	200.		sat, ADI, H	
HIP116910	HD222575	7.8	G8V	63.7	100.		sat, ADI, H	

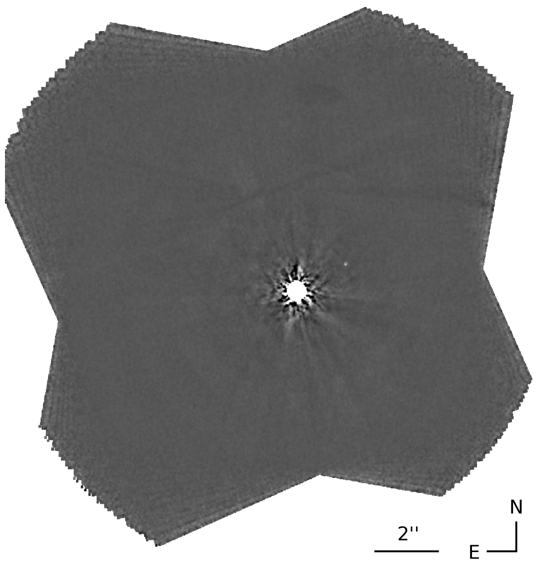

Fig. 3. VLT/NACO ADI observation in H-band combined of the young star TYC 7617-0549-1 (K0V, 76.4 pc and 30 Myr). A faint ($\Delta H = 12.7$ mag) candidate, resolved at 1.8 ″, has been finally identified as a background contaminant (see Fig. 6).

Table 5. Mean plate scale and true north orientation for each observing run of the NaCo-LP.

UT Date	Platescale (mas)	True north (deg)	Calibrator
2009-11-23	13.22 ± 0.02	-0.17 ± 0.03	θ_1 Ori C
2010-02-15	13.21 ± 0.02	-0.33 ± 0.03	IDS1307
2010-02-18	13.21 ± 0.02	-0.33 ± 0.03	θ_1 Ori C
2010-06-16	13.21 ± 0.02	-0.53 ± 0.03	IDS1307
2010-07-30	13.21 ± 0.02	-0.47 ± 0.03	IDS1307
2010-12-30	13.21 ± 0.02	-0.47 ± 0.03	θ_1 Ori C
2011-01-30	13.21 ± 0.02	-0.49 ± 0.03	θ_1 Ori C
2011-05-11	13.21 ± 0.02	-0.52 ± 0.03	IDS1307
2011-07-02	13.21 ± 0.02	-0.55 ± 0.03	IDS1307
2012-01-02	13.22 ± 0.02	-0.59 ± 0.03	IDS1307
2012-01-02	13.22 ± 0.02	-0.59 ± 0.03	θ_1 Ori C

Vigan et al. (2012), the IPAG-ADI pipeline by Chauvin et al. (2012) and the Padova-ADI pipeline by Esposito et al. (2013). Each pipeline processed the data in a similar way for the first cosmetics steps of flat-fielding, bad and hot-pixels removal, and sky-subtraction. To determine the central star position, as for the frames recentering, a Moffat fitting of the non-saturated part of the stellar PSF wing (with a similar threshold) was used. Finally, an encircled energy criteria was considered for the rejection of open-loop and poorly-corrected frames to compute a final mastercube together with the correspoding parallactic angle variation. The main differences between the pipelines mostly reside in the various ADI algorithms applied (cADI and sADI, see Marois et al. 2006; LOCI, see Lafrenière et al. 2007) and in the

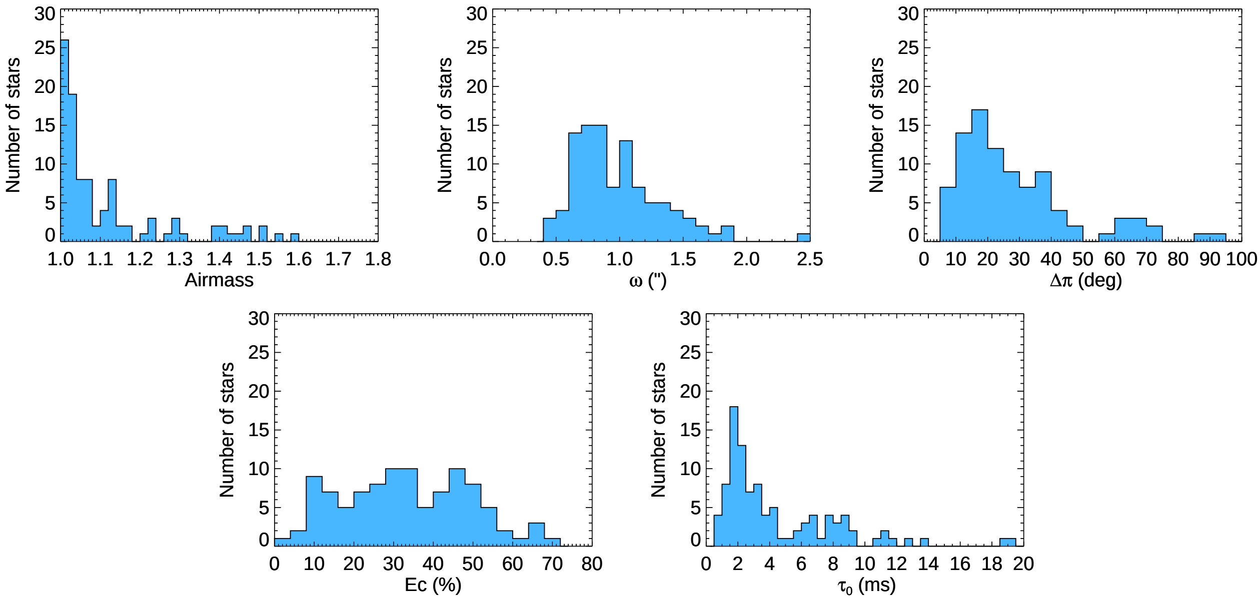

Fig. 2. Histograms summarizing the observing conditions of the NaCo-LP campaigns: airmass, DIMM seeing (ω), parallactic angle variation ($\Delta\pi$), coherent energy (Ec) and coherent time (τ_0).

parameters setup. Consistent results within 0.1–0.2 mag in photometry (candidate photometry and detection limits) and 0.2–0.3 pixels in astrometry were found between the different pipelines for a serie of targets used as test cases. Non-saturated PSFs were similarly reduced without PSF-subtraction.

The results presented in this final analysis have been obtained with the LAM-ADI pipeline using LOCI, considering optimization regions of $N_A = 300 \times FWHM$ at less than $3\,''$ and $N_A = 3000 \times FWHM$ at more than $3\,''$, the radial to azimuthal width ratio $g = 1$, the radial width $\Delta r = 2 \times FWHM$ and a separation criteria of $0.75 \times FWHM$. The binning of the data was tuned to apply LOCI on a final mastercube reduced to ~ 350 frames. An illustration of the final LOCI processed image of the young star TYC 7617-0549-1 (K0V, 76.4 pc and 30 Myr) is shown in Fig. 3.

4.2. Relative astrometry and photometry

The relative position and flux of all candidates was determined using Moffat fitting and aperture photometry corrected from the ADI flux loss. This first order analysis was sufficient to assess the candidate proper motion and nature as described in sub-section 5.2. For the most interesting cases (like HD 8049), the injection of fake planets at the location of the candidate signal was done to properly take into account any local astrometric and photometric biases induced by the ADI-processing described in Chauvin et al. (2012).

To finally calibrate the relative astrometric position of the detected candidates to the primary star, we used the θ_1 Ori C field observed with HST by McCaughrean & Stauffer (1994) (with the same set of stars TCC058, 057, 054, 034 and 026) as a primary calibrator. The astrometric binary IDS 13022N0107 (van Dessel & Sinachopoulos 1993) was then used as a secondary calibrator when the θ_1 Ori C field was not observable and then recalibrated on the θ_1 Ori C field when both were observable. Both fields were observed in standard field-stabilized mode and reduced (cosmetics, flat-fielding, bad and hot-pixels removal, sky-subtraction and recentering) using the *Eclipse*[1] reduction software developed by Devillar (1997). Finally, for ADI data, the NaCo rotator offset at the start of each ADI sequence was also calibrated and taken into account as described by Chauvin et al. (2012). The results of the platescale and true north orientation determinations are given in Table 5.

The throughput of the NaCo neutral density filter was recalibrated on sky using two different datasets taken for the star TYC 9162-0698 during our February 2010 visitor run. Using aperture photometry on the data taken with and without the neutral density, we derived a transmission factor of $1.19 \pm 0.05\%$ with the H-band filter. This result is consistent with the one derived by Bonnefoy et al. (2013a) and was used to calibrate the candidate photometry and the detection limits using the non-saturated sequence of the primary star with the neutral density filter as a photometric reference.

4.3. Detection limits determination

A pixel-to-pixel noise map of each observation was estimated within a box of 5×5 pixels sliding from the star to the limit of the NACO field of view. To correct for the flux loss related to the ADI processing, fake planets were regularly injected every 20 pixels in radius at 10 different position angles for separations smaller than $3\,''$. At more than $3\,''$, fake planets were injected every 50 pixels at 4 different position angles. The final flux loss was computed with the azimuthal average of the flux losses of fake planets at same radii. The final detection limits at 5σ were then obtained using the pixel-to-pixel noise map divided by the flux loss and normalized by the relative calibration with the primary star (considering the different exposure times and the neutral density). LOCI processing leads to residuals whose

[1] http://www.eso.org/projects/aot/eclipse/

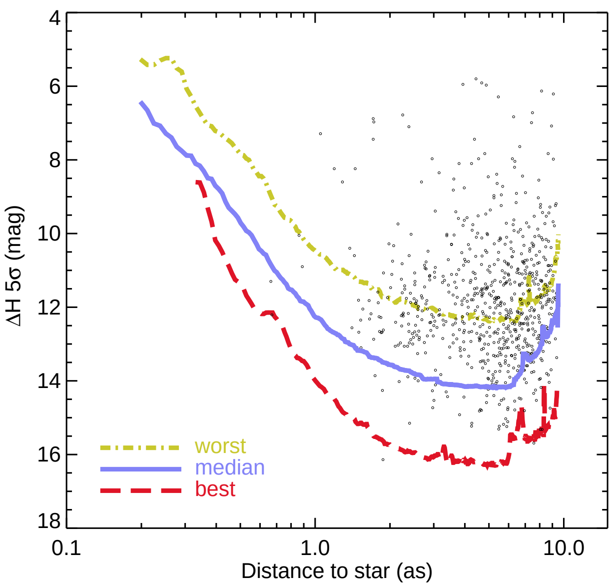

Fig. 4. VLT/NACO deep ADI 5σ detection limits in H-band combined with the S13 camera. The worst, median and best detection limits are shown with all the candidates detected. Separations of less than 0.1–0.2 $''$ are generally saturated.

distribution closely resembles a Gaussian (Lafrenière et al. 2007), therefore a 5σ threshold is thus adequate for estimating detection performances. The best, worst and median detection limits of the survey are reported in Fig. 4.

5. Results

A total of 86 sources were observed. 16 stars were resolved as binaries, including HD 8049 with a newly discovered white dwarf companion. 10 binaries were simply observed in non-saturated ADI imaging to directly derive their relative astrometry and photometry. 76 stars were observed in saturated high-contrast ADI to search for faint substellar companions. In the following sub-sections, we describe the properties of the new stellar multiple systems, the status of the detected candidates in saturated ADI, the characteristics of the white dwarf companion around HD 8049, finally the fine analysis of the thin debris-disk around HD 61005.

5.1. New stellar close multiple systems

Despite our sample selection to reject close ($0.1 - 6.0\,''$) binaries, 16 stars were resolved as multiple. Three systems were already known, HIP 108422 AB (Chauvin et al. 2003), TYC 7835-2569-1 AB (Brandner et al. 1996) and TYC 6786-0811-1 (Köhler et al. 2000), and went through our sample selection process by mistake. TYC 8484-1507-1 is actually also a known $\sim 8.6\,''$ binary that was resolved by 2MASS, not rejected during our sample selection, but resolved in the NaCo FoV despite its large separation. Then, in the case of HD 8049, the faint comoving companion turned out to be a white dwarf. Its characteristics are briefly described in Subsection 5.3). At the end, a total of 11 new close multiple systems were resolved. All of them were observed in non-saturated ADI to derive their position and H-band photometry relative to the primary star (see Table 6). The visual binaries HIP 108422 AB, TYC 7835-2569-1 AB and TYC 6786-0811-1 are confirmed as physically bound. Deep ADI observations were obtained in addition for six binaries (TYC 0603-0461-1, TYC 7835-2569-1, HD 8049, TYC 8927-3620-1, HIP 80290 and TYC 8989-0583-1).

Table 6. Relative positions and H-band contrast of the new binaries resolved during the NaCo-LP. Epochs of observation are reported in Tables 7, 8, 9, 10 and 11.

Name	Δ (mas)	PA (deg)	ΔH (mag)
HIP 8038[a]	437 ± 7	273.8 ± 0.9	2.5 ± 0.2
HIP 80290	3340 ± 4	257.5 ± 0.2	1.9 ± 0.2
HIP 94235	506 ± 7	150.6 ± 0.8	3.8 ± 0.3
HIP 107684	326 ± 7	270.2 ± 1.2	2.8 ± 0.3
HD 199058	471 ± 7	282.9 ± 0.8	2.5 ± 0.2
TYC 0603-0461-1	74 ± 14	74.2 ± 5.1	0.1 ± 0.4
TYC 8927-3620-1[b]	87 ± 14	296.8 ± 4.35	0.5 ± 0.4
TYC 8989-0583-1	2584 ± 8	169.8 ± 0.15	2.7 ± 0.2
TYC 9010-1272-1	262 ± 8	238.0 ± 1.44	1.0 ± 0.3
TYC 9181-0466-1	1891 ± 7	123.4 ± 0.2	1.5 ± 0.2
TYC 9231-1566-1	1975 ± 7	145.5 ± 0.2	3.0 ± 0.2

(a): Known binary separated by 15.0 arcsec and $\Delta V = 2.0$ mag.
(b): Third component resolved by 2MASS at $\sim 4.8''$ and $\Delta K = 0.7$ mag.

5.2. Companion candidates

Among the 76 stars observed in ADI, one companion candidate or more were detected for 43 targets (see Tables 2 and 3). More than 700 candidates were detected, 90% of them in six very crowded field (see Fig. 4). The galactic contamination rate of the NaCo-LP fields by at least one background source predicted by the Besançon galactic population model (Robin et al. 2003) is equal to 51%, in reasonable agreement with the 56% (43 systems with at least one candidate for the 76 observed). The model uses as input the NaCo field of view, the typical magnitude limit of the NaCo-LP ($H_{\rm lim} = 21$ mag) and the galactic coordinates of all targets. The repartition of these galactic contaminants is given in Fig. 5. Solar-system and extra-galactic contaminants are expected to be significantly less frequent. Moreover, solar system contaminants smear during a 1-hr observing sequence and extra-galactic contaminants are mainly extended background galaxies resolved by NaCo. The most important population of contaminants that can mimic the apparent flux of giant planet or brown dwarf companions bound to the star are M dwarfs with typical $H = 20 - 22$ mag apparent magnitudes.

To identify their nature, we relied on the follow-up observations at additional epochs to distinguish comoving companions from stationary background stars. The candidates were ranked by priority as a function of their predicted masses (higher priority to lower masses), projected physical separations (assuming they would be bound; higher priority to closer candidates) and predicted false alarm probabilities using the Besançon galactic population model (Robin et al. 2003) to guide the follow-up strategy. Follow-up observations with a second epoch were obtained

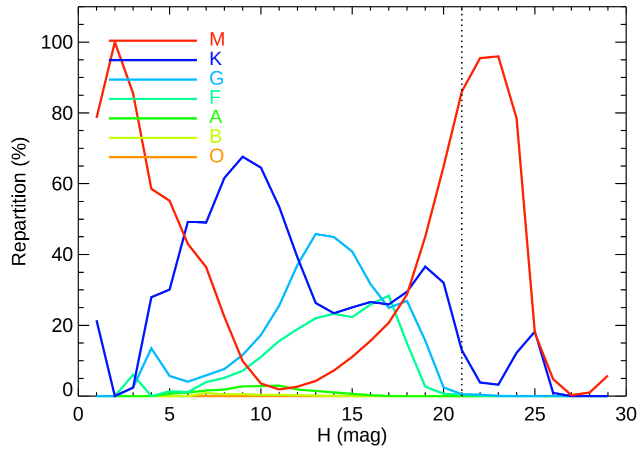

Fig. 5. Expected spectral type distribution of field stars from the Besançon galactic population model observed during the NaCo-LP. The FoV, the typical magnitude limit of the NaCo-LP ($H_{\rm lim} = 21$ mag) and the galactic coordinates of all targets were considered. The predicted repartion is given as a function of the spectral type and the apparent magnitude in H-band.

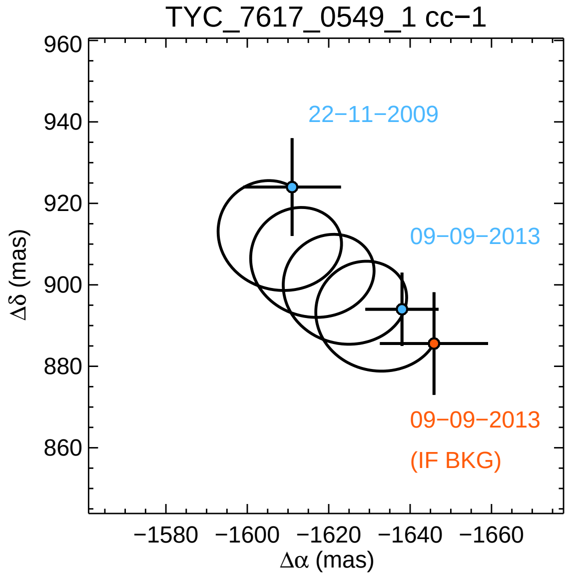

Fig. 6. VLT/NaCo measurements (filled circles with uncertainties) of the offset positions of the companion candidate to TYC 7617-0549-1 (see Fig. 3). The expected variation of offset positions, if the candidate is a background object, is shown (curved line). The variation is estimated based on the parallactic and proper motions of the primary star, as well as the initial offset position of the companion candidate from TYC 7617-0549-1. The companion candidate is clearly identified here as a stationary background contaminant.

for 29 targets, including the Moth system (HD 61005) characterized during dedicated follow-up observations. The amplitude of stellar proper motion (larger than 30 mas/yr for 80% of the NaCo-LP target) enabled a rapid identification over 1 yr interval (see Fig. 1, *Bottom-Middle*).

For the 29 systems with at least 2-epochs observations (including the Moth system), we used a χ^2 probability test of $2\times N_{epochs}$ degrees of freedom (corresponding to the measurements: separations in the $\Delta\alpha$ and $\Delta\delta$ directions for the number N_{epochs} of epochs). This test takes into account the uncertainties in the relative positions measured at each epoch and the uncertainties in the primary proper motion and parallax (or distance). Fig. 6 gives an illustration of a ($\Delta\alpha$, $\Delta\delta$) diagram that was used to identify a stationary background contaminant around TYC 7617-0549-1. A status has been assigned to each candidate as background contaminant (B; $P_{{\rm comoving},\chi^2} < 1\%$ and with a relative motion compatible with a background source), comoving (C; $P_{{\rm BKG},\chi^2} < 1\%$) and with the relative motion compatible with a comoving companion) and undefined (U) when observed at only one epoch or when not satisfying the first two classifications.

Only one comoving companion was identified, the white dwarf companion around HD 8049 described here after. Among the 28 other follow-up fields, 10 fields have been completely characterized and 18 partially owing to detection limits variation from one epoch to another. 14 fields still require second epoch observations. The status of all the candidates is given in Tables 7, 8, 9, 10 and 11.

5.3. A white dwarf companion around HD 8049

The only comoving companion identified in this survey, with a preliminary predicted mass of 35 $M_{\rm Jup}$, was discovered around the star HD 8049 (K2, 33.6 pc). The star had a predicted age of 90–400 Myr from its rotational period, H&K emission and X-ray emission. Thanks to the high proper motion of the central star ($\mu_\alpha = 65.99\pm1.18$ mas/yr and $\mu_\delta = 240.99\pm0.98$ mas/yr), a χ^2 probability test on $\Delta\alpha$ and $\Delta\delta$ with respect to the star at two epochs rejected the possibility (at 99% certainty) that the object was a background source. Further analysis using archived data, radial velocity observations spanning a time range of $\sim$ 30 yr, U-band imaging with EFOSC and near-infrared spectroscopy of the comoving companion with VLT/SINFONI finally revealed that the companion was actually a white dwarf (WD) with temperature $T_{\rm eff} = 18800 \pm 2100$ K and mass $M_{\rm WD} = 0.56 \pm 0.08$ $M_\odot$.

This astrophysical false positive revealed that the system age was much older than initially thought. The age diagnostics have likely been affected as the central star has been probably rejuvenated by the accretion of some amount of mass and angular momentum at the time of mass loss from the WD progenitor. A complete analysis of the system (evolution, kinematics) by Zurlo et al. (2013) actually reveals that the resulting age of the system is about 3–6 Gyr.

5.4. The Moth resolved as a thin debris-disk

In the course of the survey, the emblematic star HD 61005 (G8V, 90 Myr, 34.5 pc), known to host The Moth debris disk (Hines et al. 2007), was observed. The NaCo H-band image remarkably resolves the disk component as a distinct narrow ring at inclination of $i = 84.3 \pm 1.0^o$, with a semimajor-axis of $a = 61.25 \pm 0.85$ AU and an eccentricity of $e = 0.045 \pm 0.015$. The observations also revealed that the the ring center is offset from the star by at least 2.75 ± 0.85 AU indicating a possibly dynamical perturbation by a planetary companion that perturbs the remnant planetesimal belt. The observations and the detailed disk modeling was published by Buenzli et al. (2010). Subsequent observations did not reveal any giant planet companions. Three other stars of our sample are known to host debris-disks: HIP 11360 (HD 15115; Kalas et al. 2007, Rodigas et al. 2012), HIP 99273 (HD 191089; Churcher et al. 2011) and HIP 76829 (HD 139664; Kalas et al. 2006). No clear detection was obtained with our ADI analysis.

6. Survey's statistical analysis

6.1. Sample definition

To define a meaningful sample for the statistical analysis of the survey, we first removed from the sample of 76 stars observed in ADI all visual and spectroscopic binaries, including the six visual multiple systems observed in that mode (TYC 0603-0461-1, TYC 7835-2569-1, HD 8049, HIP 8290, TYC 8927-3620-1 and TYC 8989-0583-1) and 7 new spectroscopic binaries unknown at the time of our sample selection. We have then selected two sub-samples:

- the *full-stat* sample of 63 stars including all single stars observed in ADI with detection sensitivities down to planetary masses for physical separations ranging from 10 to 2000 AU. The status of all the candidates detected in these fields have however not been fully completed, although a large majority are expected to be stationary background contaminants. This sample gives an estimation of the ultimate performances of the survey interms of masses and physical separations when the candidate status identification will be complete, probably with SPHERE in the forthcoming years.
- the *complete-stat* sample of 51 stars has been restreined to all systems for which the candidate status identification was complete up-to 300 AU, including cases with no companion candidates detected or with companion candidates properly identified thanks to our follow-up observations as stationary background sources or comoving companions. In the case of follow-up observations with variable detection performances from one epoch to another (therefore with possible undefined faint sources due to the lack of redetection), only the worst detection limit was considered. These selection criteria offered us at the end a meaningful sample for which the detection and the status identification of the candidates was complete.

6.2. Survey detection probability

To correct for the projection effect from the observations, we then ran a set of Monte-Carlo simulations using an optimized version of the MESS code (Bonavita et al. 2012). For the *full-stat* sample, the code generates a uniform grid of mass and semi-major axis in the interval [1, 75] $\mathrm{M_{Jup}}$ and [1, 2000] AU with a sampling of 0.5 $\mathrm{M_{Jup}}$ and 1 AU between 1 and 1000 AU, and 2 AU between 1000 and 2000 AU. For the *complete-stat* sample, the uniform grid is generated in the semi-major axis range between [1, 300] AU with a sampling of 1 AU. For each point in the grids, 100 orbits were generated, randomly oriented in space from uniform distributions in sin(i), ω, Ω, $e \leq 0.8$, and T_p. The on-sky projected position (separation and position angle) at the time of the observation is then computed for each orbit and compared to our 5σ 2D-detection maps to determine the individual detection probability (p_j) of planets around each star. The average of all individual detection limits gives us the typical mean detection probability ($< p_j >$) of the NaCo-LP to the planet and BD companion population. The results for the *full-stat* and *complete-stat* samples are shown in Fig. 7 and 8 *Top*) respectively. The detection probabilities in both cases do not significantly differ at less than 300 AU. Most companions more massive than 20 $\mathrm{M_{Jup}}$ with semi-major axis between 70 and 200 AU should have been detected during our survey. We are 50% sensitive to massive (≥ 10 $\mathrm{M_{Jup}}$) planets and brown dwarfs with semi-major axis between 60 and 400 AU. Finally, the detection of giant planets as light as 5 $\mathrm{M_{Jup}}$ between 50-800 AU is only possible for 10% of the stars observed. The relatively small number of very young stars (see Fig. 1) is responsible for this limited sensitivity to light giant planets.

6.3. Giant planet occurrence at wide orbits

To derive the occurrence of giant planets and brown dwarfs in our survey, we only considered the *complete-stat* sample with a complete census of the candidates status within 300 AU. As no planetary mass or brown dwarf companions were detected, we considered here a null-detection result. We then used the mean detection probability ($< p_j >$) to derive the giant planet and brown dwarf occurrence upper limit ($f_{\max}$) compatible with the survey detection limits. The probability of planet detection for a survey of N stars is described by a binomial distribution, given a success probability $f p_j$ with f the fraction of stars with planets. p_j is the individual detection probability of detecting a planet if present around the star j and computed previously. Assuming that the number of expected detected planets is small compared to the number of stars observed, the binomial distribution can be approximated by a Poisson distribution to derive a simple analytical solution for the exoplanet fraction upper limit ($f_{\max}$). The formalism is described by Carson et al. (2006) and Lafrenière et al. (2007). The result is shown in Fig. 8 (*Bottom-Left* and *Bottom-Right*). For this *complete-stat* sample, we constrain the occurrence of exoplanets more massive than 5 $\mathrm{M_{Jup}}$ to typically less than 15% between 100 and 300 AU, and less than 10% between 50 and 300 AU for exoplanets more massive than 10 $\mathrm{M_{Jup}}$ considering a uniform input distribution and with a confidence level of 95%. These values are consistent with current estimations from various studies with comparable sensitivities around young, solar-type stars (**$f_{\max} \leq 9.7\%$ for $[0.5, 13]$ $\mathrm{M_{Jup}}$ planet between $[50-250]$ AU by Lafrenière et al. 2007; $f_{\max} \leq 10\%$ for $[1, 13]$ $\mathrm{M_{Jup}}$ planet between $[40-150]$ AU Chauvin et al. 2010; $f_{\max} \leq 6\%$ for $[1, 20]$ $\mathrm{M_{Jup}}$ planet between $[10-150]$ AU by Biller et al. 2013**).

A more complete analysis combining the results of the NaCo-LP with archive data for a total of ~ 210 stars already observed in direct imaging, will be presented in the related papers by Vigan et al. (2014, in prep) and Reggiani et al. (2014, in prep). These analysis will provide significant and relevant statistical constraints on the population of planets and brown dwarfs around young, nearby solar-type (FGK) stars (single or members of wide binaries) and enable tests of planet and brown dwarf formation models.

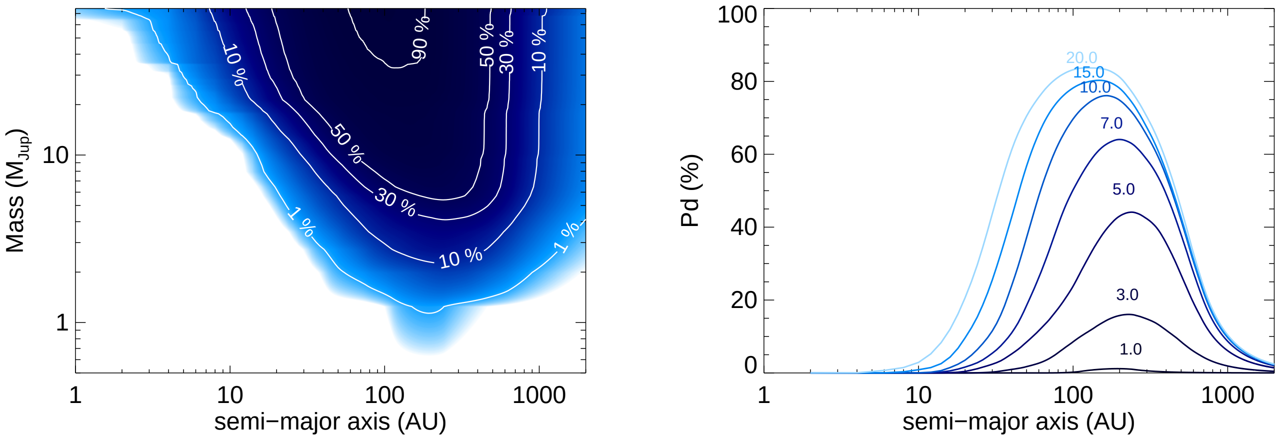

Fig. 7. *Left:* NaCo-LP mean detection probability map ($< p_j >$) as a function of the mass and semi-major axis. *Right:* Mean probability curves for different masses (1, 3, 5, 7, 10, 15 and 20 M_{Jup}) as a function of the semi-major axis.

7. Conclusion

In the context of the scientific preparation of the VLT/SPHERE guaranteed time, we have conducted a survey of 86 young, nearby and mostly solar-type stars using NaCo at VLT between 2009 and 2013. Our main goals were to detect new giant planets and brown dwarf companions and to initiate a relevant statistical study of their occurrence at wide ($10 - 2000$ AU) orbit. NaCo was used in pupil-stabilized mode to perform angular differential imaging at H-band. It enables us to reach contrast performances as small as 10^{-6} at $1.5''$. Over the 86 stars observed, the survey led to:

- the discovery of 11 new close binaries that we characterized in terms of relative photometry and astrometry.
- the detection of more than 700 companion candidates, 90% of them being located in six crowded fields. Among 76 stars observed in deep ADI, 33 systems have no point-source detected in their vicinity and 43 systems have at least one companion candidate detected. Repeated observations at several epochs enabled us to analyze the candidate status, completely or partially, around 29 stars. Planetary mass candidates with proper follow-up were all identified as background sources. Additional follow-up observations will still be necessary to fully complete the status identification of all candidates detected in the survey owing to the variability of the detection performances from one run to another. It shows that more than two epochs is generally necessary during a survey for a full exploration of the companions content.
- the discovery of a unique comoving companion to the star HD 8049. This result has been published by Zurlo et al. (2013) and revealed that the companion was actually a white dwarf with temperature $T_{\rm eff} = 18800 \pm 2100$ K and mass $M_{\rm WD} = 0.56 \pm 0.08\ M_\odot$.
- new high-contrast images of the Moth debris-disk at HD 61005. The NaCo *H*-band image remarkably resolves the disk component as a distinct narrow ring offset from the star by at least 2.75 ± 0.85 AU indicating a possibly dynamical perturbation by a planetary companion. This study was published by Buenzli et al. (2010).
- finally, a preliminary statistical analysis of the survey detection probabitlities around the sample of 63 young, single and mostly solar-type (FGK) stars observed in angular differential imaging, i.e with detection performances enabling the search for planets and brown dwarfs in the stellar environment. Most companions more massive than 20 M_{Jup} with semi-major axis between 70 and 200 AU should have been detected during our survey. We are 50% sensitive to massive ($\geq 10\ M_{Jup}$) planets and brown dwarfs with semi-major axis between 60 and 400 AU. Finally, the detection of giant planets as light as 5 M_{Jup} between 50-800 AU is only possible for 10% of the stars observed. We have then defined a more complete sample of 51 stars restreined to all systems for which the candidate status identification was complete up-to 300 AU, including cases with no companion candidates detected or with companion candidates properly and completely identified. Based on this complete sample average detection probability, a non-detection result and considering a uniform distribution of giant planets and brown dwarf companions in terms of semi-major axis and mass, we derive a typical upper limit for the occurrence of exoplanets more massive than 5 M_{Jup} of 15% between 100 and 300 AU, and 10% between 50 and 300 AU for EPs more massive than 10 M_{Jup} with a confidence level of 95%.

Combined with compiled archived data, the results of this survey offer a unique sample of $\sim$ 210 young, solar-type stars observed in deep imaging to constrain the presence of giant planets and brown dwarfs in their close environment. A more complete statistical analysis will be published in two linked articles by Vigan et al. (2014, in prep) and Reggianni et al. (2014, in prep) to test the relevance of various analytical distributions to describe the giant planet and brown dwarf companion population at wide orbits, but also to bring further constraints on current theories of planetary formation. All final products of this survey (images, detection limits and candidate status) will be released in the *DIVA* (*Deep Imaging Virtual Archive*) database, together with the archive data used for full statistical analysis. We encourage the community to support this effort by sharing the final products (reduced images, detection limits

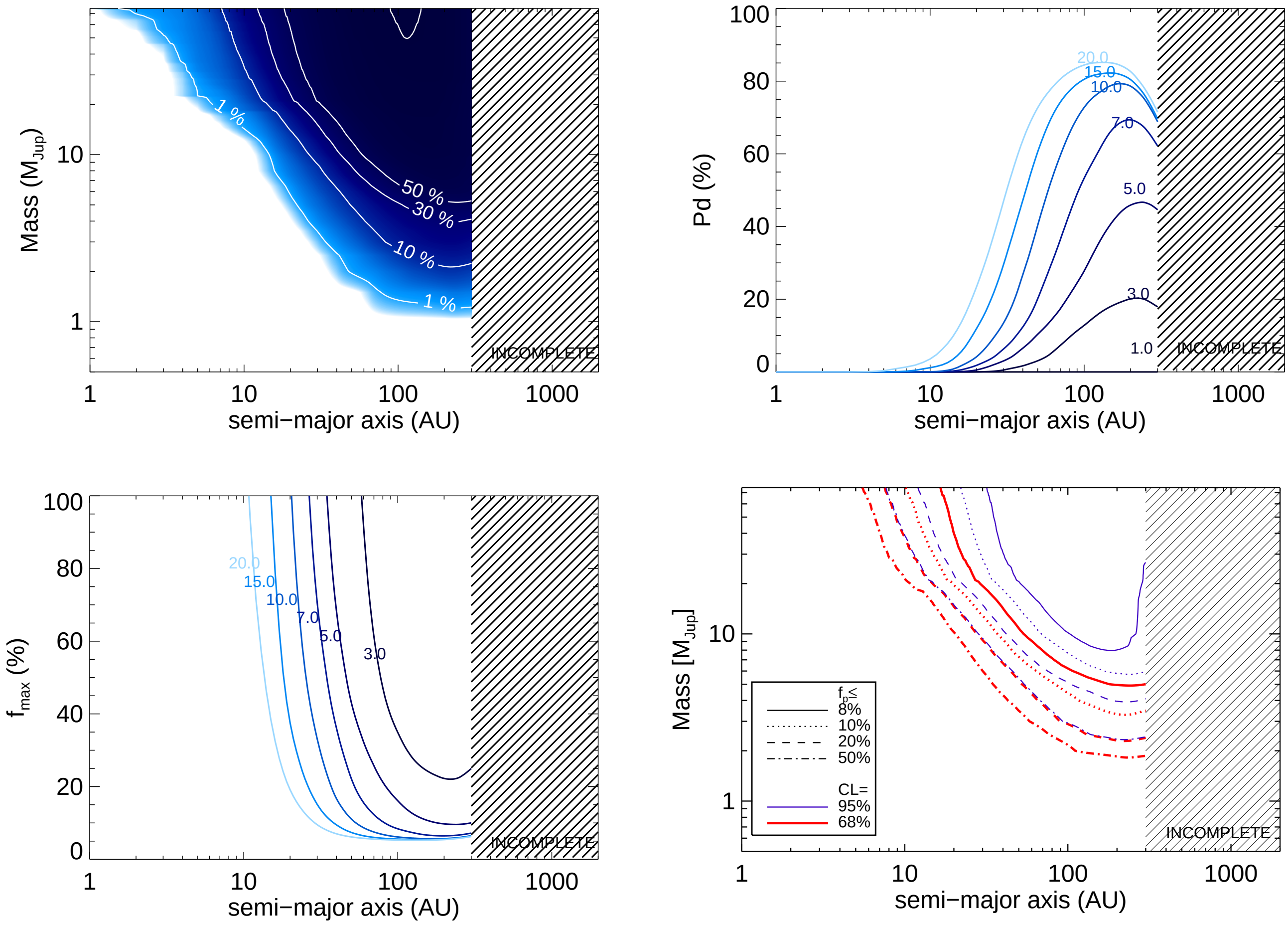

Fig. 8. Results for the *complete-stat* sample. *Top-Left:* NaCo-LP mean detection probability map ($< p_j >$) as a function of the mass and semi-major axis. *Top-Right:* Mean probability curves for different masses (1, 3, 5, 7, 10, 15 and 20 M_{Jup}) as a function of the semi-major axis. *Bottom-Left:* Giant planet and brown dwarf occurrence upper limit (f_{max}), considering a 95% confidence level, for different masses (3, 5, 7, 10, 15 and 20 M_{Jup}) as a function of the semi-major axis considering the null-detection result and an uniform distribution of planets and brown dwarfs in terms of masses and semi-major axis. *Bottom-Right:* Same occurrence upper limit (f_{max}) expressed this time in a mass versus semi-major axis diagramme for a 68% and 95% confidence level (following Biller et al. 2007; Nielsen et al. 2008 representation).

and candidate relative astrometry, photometry and status) of their published surveys to optimally prepare the future of planet imaging searches coming with the new generation of planet imagers like LMIRCam, MagAO, SPHERE, GPI, SCExAO and in a longer term JWST (Clampin 2010), TMT-PFI (Simard et al. 2010) and EELT-MIR and EELT-PCS (Brandl et al. 2010; Kasper et al. 2010).

Acknowledgements. We greatly thank the staff of ESO-VLT for their support at the telescope. This publication has made use of the SIMBAD and VizieR database operated at CDS, Strasbourg, France. Finally, we acknowledge supports from: 1) the French National Research Agency (ANR) through project grant ANR10-BLANC0504-01 and the *Programmes Nationaux de Planétologie et de Physique Stellaire* (PNP & PNPS), in France for G.C., A.V, P.D., J-L. B., A-M. L. and D.M., 2) INAF through the PRIN-INAF 2010 Planetary Systems at Young Ages project grant for S.D., D.M., M.B. and R.G. and 3) the U.S. National Science Foundation under Award No. 1009203 for J.C.

References

Alibert Y., Mordasini C. & Benz W. 2004, A&A, 417, L25
Apai D., Janson M., Moro-Martín A. et al. 2008, ApJ, 672, 1196
Baraffe I., Chabrier G., Gallardo J. 2009, A&A, 702, 27
Barman T.S., Macintosh B., Konopacky Q.M. & Marois C. 2011a, ApJ, 733, 65
Barman T.S., Macintosh B., Konopacky Q.M. & Marois C. 2011b, ApJ, 735, L39
Batalha N.M., Rowe J.F., Bryson S.T. et al. 2013, ApJS, 204, 24
Beuzit J.-L., Feldt M., Dohlen K. et al. 2008, SPIE, 7014, 41
Biller B.A., Close L.M., Masciadri E. et al. 2007, ApJS, 173, 143
Biller E., Liu M., Wahhaj Z. et al. 2013, ApJ, accepted, arXiv:1309.1462
Boley A.C. 2009, ApJ, 695, L53
Boley A.C., Hayfield T., Mayer L. & Durisen R.H. 2010, Icarus, 207, 509
Bonavita M., Chauvin G., Desidera S. et al. 2012, A&A, 537, 67
Bonfils X., Delfosse X., Udry S. et al. 2013, A&A, 549, 109
Bonnefoy M., Chauvin G., Lagrange A.M. et al. 2010, A&A, 512, 52
Bonnefoy M., Boccaletti A., Lagrange A.M. et al. 2013a, A&A, 555, 107
Bonnefoy M., Chauvin G., Lagrange A.M. et al. 2013b, A&A, accepted, arXiv:1306.3709
Bonnefoy M., Currie M., Marleau G.D. et al. 2013c, ApJ, accepted, arXiv:1308.3859
Boss A.P. 1997, Science, 276, 1836
Bowler B., Liu M., Dupuy T.J. & Cushing M.C. 2010, ApJ, 723, 850
Brandl B.R., Lenzen R., Pantin E. et al. 2010, SPIE, 7735, 83

Brandner W., Alcala J. M., Kunkel M., Moneti A. & Zinnecker H. 1996, A&A, 307, 121
Brandt T., Kuzuhara M., McElwain M.W. et al. 2013, ApJ, submitted, arXiv:1305.7264
Buenzli E., Thalmann C., Vigan A. et al. 2010, A&A, 524, L1
Carson J., Eikenberry S.S., Smith J.J. & Cordes J.M. 2006, AJ, 132, 1146
Carson J., Thalmann C., Janson M. et al. 2013, ApJ, 763, L32
Chauvin G., Thomson M., Dumas C. et al. 2003, A&A, 404, 157
Chauvin G., Lagrange A.-M., Zuckerman B. et al. 2005a, A&A, 438, L29
Chauvin G., Lagrange A.-M., Dumas C. et al. 2005b, A&A, 438, L25
Chauvin G., Lagrange A.-M., Bonavita M. et al. 2010, A&A, 509, 52
Chauvin G., Lagrange A.-M., Beust H. et al,, 2012, A&A, 542, 41
Churcher L., Wyatt M. & Smith R. 2011, MNRAS, 410, 2
Clampin M. 2010, Pathways Towards Habitable Planets, ASP Conference Series, Vol. 430, 2010
Close L., Males J.R., Kopon D.A. et al. 2012, SPIE, 8447, 0
Delorme P., Lagrange A.-M., Chauvin G. et al. 2012, A&A, 539, 72
Devillar N. 1997, Messenger, 87
Esposito S., Mesa D., Skemer A. et al. 2013, A&A, 549, 52
Dawson R.I. & Murray-Clay R.A. 2013, ApJ, 767, L24
Forgan D. & Rice K. 2013, MNRAS, 432, 3168
Guyon O., Martinache F., Garrel V. et al. 2010, SPIE, 7736, 71
Heinze A.N., Hinz P.M., Sivanandam S. et al. 2010, ApJ, 714, 1551
Heinze A.N., Hinz P.M., Kenworthy M. et al. 2010, ApJ, 714, 1570
Hines D.C., Schneider G., Hollenbach D. et al. 2007, ApJ, 671, L165
Hoff W., Henning T. & Pfau W. 1998, A&A, 336, 242
Howard A.W., Johnson J.A., Marcy G.W. 2010, ApJ, 721, 1467
Howard A.W., Marcy G.W., Bryson S.T. 2012, ApJ, 201, 15
Janson M., Bergfors C., Goto M., Brandner W. & Lafrenière D. 2010, ApJ, 710, L35
Janson M., Bonavita M., Klahr H. et al. 2013, ApJ, 736, 89
Janson M., Brandt T. D., Moro-Martín A. et al. 2013, ApJ, 773, 73
Joergens V., Bonnefoy M., Liu Y. et al. 2013, A&A, 558, L7
Kalas P., Graham J. R., Clampin M.C. & Fitzgerald M. P. 2006, ApJ, 637, L57
Kalas P., Fitzgerald M. P. & Graham J. R. 2007, ApJ, 661, L85
Kalas P., Graham J.R., Chiang E. et al. 2008, Science, 322, 1345
Kalas P., Graham J.R., Fitzgerald M.P. & Clampin M. 2013, ApJ, 775, 56
Kasper M., Apai D., Janson M. & Brandner W. 2007, A&A, 472, 321
Kasper M., Beuzit J.-L., Vérinaud C. et al. 2010, SPIE, 7735, 81
Kastner J.H., Zuckerman B., Weintraub D.A. & Forveille T. 1997, Science, 277, 67
Kley W. & Nelson R.P. 2012, ARA&A, 50, 211
Yamamoto K., Matsuo T., Shibai H. et al. 2013, PASJ, accepted, arXiv:1306.3100
Köhler R., Kunkel M., Leinert C. & Zinnecker H. 2000, A&A, 356, 541
Konopacky Q. M., Barman T. S., Macintosh B. A. & Marois, C. 2013, Science, 339, 1398
Kuzuhara M., Tamura M., Kudo T. et al. 2013, ApJ, 774, 11
Lafrenière D., Doyon R., Marois C. et al. 2007, ApJ, 670, 1367
Lafrenière D., Jayawardhana R., van Kerkwijk M.H. et al. 2008, ApJ, 689, 153
Lagrange A.-M., Gratadour D., Chauvin G. et al., 2009, A&A, 506, L972
Lambrechts M. & Johansen A. 2012, A&A, 544, L32
Lenzen R., Hartung M., Brandner et al. 2002, SPIE, Vol. 4841
Liu M.C., Magnier E.A., Deacon N.R. et al. 2013, ApJ, 777, L20
Lowrance P.J., Becklin E.E., Schneider G. et al. 2005, AJ, 130, 1845
Luhman K. 2012, ARA&A, 50, 65
Macintosh B., Graham J.R., Palmer D. et al. 2008, SPIE, 7015, 31
Marois C., Lafrenière D., Doyon R., Macintosh B. & Nadeau D. 2006, ApJ, 641, 556
Marois C., Macintosh B., Barman T., et al.,2008, Science 322, 1348
Marois C., Zuckerman B., Konopacky Q.M., Macinosh B. & Barman T., 2010, Nature 468, 1080
Masciadri E., Mundt R., Henning Th. & Alvarez C. 2005, ApJ, 625, 1004
Mayor M., Marmier M., Lovis C. et al. 2011, A&A, arXiv:1109.2497
McCaughrean M.J., Stauffer J.R. 1994, AJ, 108, 1382
Morbidelli A. & Nesvorny D. 2012, A&A, 546, 18
Naoz S., Farr W.M., Lithwick Y., Rasio F.A. & Teyssandier J. 2011, Nature, 473, 187
Nayakshin S. 2010, MNRAS, 402, 789
Neuhäuser R., Guenther E.W., Alves J. et al. 2003, AN, 324, 535
Nielsen E., Liu M., Wahhaj Z. et al. 2013, ApJ, accepted, arXiv:1306.1233
Pollack J.B., Hubickyj O., Bodenheimer P. et al. 1996, Icarus, 124, 62
Rameau J., Chauvin G., Lagrange A.-M. et al. 2013a, ApJ, 772, L15
Rameau J., Chauvin G., Lagrange A.-M. et al. 2013b, ApJ, accepted, arXiv:1310.7483
Rameau J., Chauvin G., Lagrange A.-M. et al. 2013c, A&A, 553, 60
Robin A.C., Reylé C., Derrière S. & Picaud S 2003, A&A, 409, 523
Rodigas T. J., Hinz P. M., Leisenring J. et al. 2012, ApJ, 752, 57
Rousset G., Lacombe F., Puget P., et al., 2002, SPIE, Vol. 4007
Skrutskie M.F., Jones T., Hinz P. et al. 2010, SPIE, 7735, 118
Simard L., Crampton D., Ellerbroek B. & Boyer C. 2010, SPIE, 7735, 70
Stamatellos D. & Withworth A.P. 2008, A&A, 480, 879
Torres C.A.O., Quast G.R., Melo C.H.F.
Udry S. & Santos N. C. 2007, ARA&A, 45, 397
van Dessel E. & Sinachopoulos D. 1993, A&AS, 100, 517
Vigan A., Patience J., Marois C. et al. 2012, 544, 9
Vorobyov E. I. 2013, A&A, 552, 129
Wahhaj Z., Liu M., Nielsen E.L. et al. 2013, ApJ, 773, 179
Whitworth A., Bate M.R., Nordlund A., Reipurth B. & Zinnecker H. 2007, PPV conference, University of Arizona Press, Tucson, 951 pp., 2007., p.459-476
Wright H.S., Marcy G.W., Howard A.W. et al. 2012, ApJ, 753, 160
Zapatero Osorio M.R., Béjar V.J.S., Martín E.L. 2000, Science, 290, 103
Zuckerman B. & Song I. 2004, ARAA, 42, 685
Zurlo A., Vigan A., Hagelberg J. et al. 2013, A&A, 554, 21

Table 7. Companion candidates characterization and identification (for multi-epoch observations). Target nameand observing date are given, as well as the different sources identified with their relative position and relative flux, and their identification status based on follow-up observations. Sources are indicated as: stationary background contaminants (B; based on a comoving companion probability $P_{comoving,\chi^2} < 1\%$ and with a relative motion compatible with a background source); confirmed comoving companions (C; based on a stationary background contaminant probability $P_{BKG,\chi^2} < 1\%$ and a relative motion compatible with a comoving companion); and undefined (U; when observed at only one epoch or when not satisfying the first two classifications).

Name-1	UT-Date	Candidate	Sep (mas)	PA (deg)	ΔH (mag)	Status	Comments
TYC 5839-0596-1	2009-11-24	none					SB2
TYC 0603-0461-1	2009-11-24	none					New binary (see Table 6)
HIP3924	2009-11-22	none					SB2
HIP6177	2010-07-31	cc-1	1566 ± 6	118.4 ± 0.2	7.1 ± 0.1		
	2011-07-28	cc-1	1565 ± 10	118.0 ± 0.4		C	White dwarf companion
HIP8038	2010-07-31	none					New binary (see Table 6)
HIP10602	2009-11-24	none					A few exposures
	2010-07-30	none					
HIP11360	2009-11-23	none					
TYC 8484-1507-1	2010-07-31	none					Known ($\sim 8.6'$) binary resolved by 2MASS
HIP12394	2009-11-22	none					
HIP13008	2011-09-29	cc-1	1710 ± 7	347.3 ± 0.2	6.9 ± 0.0	U	
HIP14684	2010-07-30	cc-1	5454 ± 13	150.6 ± 0.1	10.7 ± 0.1	B	
	2011-12-23	cc-1	5274 ± 6	150.3 ± 0.1	11.1 ± 0.1	B	
TYC 8060-1673-1	2009-11-23	none					
HIP19775	2009-11-22	none					
HIP23316	2009-11-23	none					
HD32981	2009-11-24	none					
BD-09-1108	2009-11-22	none					
HIP25434	2010-02-17	cc-1	4944 ± 11	154.5 ± 0.1	11.4 ± 0.1	B	
	2010-12-05	cc-1	4937 ± 5	154.5 ± 0.1	12.0 ± 0.1	B	
	2012-11-21	cc-1	4947 ± 7	155.1 ± 0.1	11.1 ± 0.1	B	
TYC 9162-0698-1	2010-02-19	26					Electronic table
	2011-01-24	26 + 33				B+U	Electronic table
TYC 5346-132-1	2009-11-23	cc-1	6252 ± 16	1.8 ± 0.2	9.7 ± 0.1	B	
	2010-02-16	cc-1	6260 ± 9	1.7 ± 0.1	9.8 ± 0.1	B	
	2009-11-23	cc-2	6431 ± 16	0.2 ± 0.2	9.1 ± 0.1	B	
	2010-02-16	cc-2	6434 ± 9	0.0 ± 0.1	9.1 ± 0.1	B	
HIP30261	2009-11-23	none					
TYC 7617-0549-1	2009-11-21	cc-1	1848 ± 16	299.6 ± 0.5	12.6 ± 0.1	B	
	2012-11-22	cc-1	1861 ± 8	298.6 ± 0.3	12.1 ± 0.1	B	
TYC 9181-0466-1	2010-02-19	none					New binary (see Table 6)
HIP32235	2010-02-18	cc-1	5559 ± 12	340.3 ± 0.2	11.8 ± 0.1	B	
	2010-12-30	cc-1	5508 ± 6	339.8 ± 0.1	13.3 ± 0.2	B	
HIP35564	2009-11-22	cc-1	1865 ± 20	304.2 ± 0.6	15.3 ± 0.3	B	RV var
	2011-01-31	cc-1	1852 ± 8	299.3 ± 0.2	14.4 ± 0.7	B	
	2009-11-22	cc-2	3301 ± 20	148.9 ± 0.3	12.4 ± 0.1	B	
	2010-02-16	cc-2	3365 ± 13	148.7 ± 0.2	12.1 ± 0.1	B	
	2011-01-31	cc-2	3465 ± 9	149.8 ± 0.2	11.9 ± 0.1	B	
	2009-11-22	cc-3	6722 ± 20	1.5 ± 0.2	14.4 ± 0.3	B	
	2010-02-16	cc-3	6660 ± 12	1.8 ± 0.2	14.0 ± 0.4	B	
	2011-01-31	cc-3	6581 ± 8	1.7 ± 0.1	13.7 ± 0.4	B	
TYC 8128-1946-1	2009-11-21	cc-1	5521 ± 17	178.2 ± 0.2	13.5 ± 0.1	B	
	2011-01-20	cc-1	5549 ± 12	178.1 ± 0.2	13.7 ± 0.2	B	
	2009-11-21	cc-2	8211 ± 17	6.3 ± 0.2	9.4 ± 0.1	B	
	2011-01-20	cc-2	8190 ± 12	6.3 ± 0.1	9.9 ± 0.1	B	
HIP36414	2010-02-17	cc-1	8296 ± 21	305.0 ± 0.2	12.8 ± 0.7	B	SB, RV var
	2011-01-31	cc-1	8241 ± 16	304.5 ± 0.1	13.5 ± 0.2	B	
	2010-02-17	cc-2	7076 ± 19	359.2 ± 0.2	13.6 ± 0.2	U	
HIP36948	2010-02-16	cc-1	3485 ± 21	327.1 ± 0.3	14.1 ± 0.2	B	The Moth[a]
	2010-02-16	cc-2	6272 ± 22	315.5 ± 0.2	13.6 ± 0.2	B	
	2010-02-16	cc-3	7217 ± 20	191.3 ± 0.2	13.3 ± 0.4	B	
	2010-02-16	cc-4	8116 ± 20	171.1 ± 0.2	14.1 ± 0.8	B	
	2010-02-16	cc-5	8206 ± 20	268.1 ± 0.2	10.1 ± 0.1	B	
HIP37563	2010-02-18	none					

(a): All background objects identified combining NaCo with HST data by Buenzli et al. (2010)

Table 8. Companion candidates characterization and identification (for multi-epoch observations). Table 7-cont.

Name-1	UT-Date	Nb Cand.	Sep (mas)	PA (deg)	ΔH (mag)	Status	Comments
HIP37923	2010-02-18	cc-1	5439 ± 10	261.2 ± 0.2	12.6 ± 0.1	B	
	2011-01-01	cc-1	5439 ± 8	259.8 ± 0.1	12.7 ± 0.1	B	
	2010-02-18	cc-2	5834 ± 12	55.5 ± 0.1	14.0 ± 0.1	B	
	2011-01-01	cc-2	5765 ± 10	56.5 ± 0.1	14.2 ± 0.2	B	
	2010-02-18	cc-3	5997 ± 12	209.9 ± 0.1	12.4 ± 0.1	B	
	2011-01-01	cc-3	6098 ± 10	209.1 ± 0.1	12.7 ± 0.1	B	
	2010-02-18	cc-4	7070 ± 12	28.2 ± 0.1	14.1 ± 0.3	B	
	2011-01-01	cc-4	6947 ± 10	28.8 ± 0.1	14.4 ± 0.2	B	
	2010-02-18	cc-5	8076 ± 13	65.1 ± 0.1	9.1 ± 0.1	B	
	2011-01-01	cc-5	8029 ± 10	65.9 ± 0.1	9.6 ± 0.1	B	
	2010-02-18	cc-6	8677 ± 15	43.1 ± 0.1	13.8 ± 0.2	U	
TYC 8927-3620-1	2010-02-19	none					New binary (see Table 6) Third component at $\sim 4.8''$ resolved by 2MASS
HIP46634	2009-11-24	none					
HIP47646	2010-02-18	none					
TWA-21	2010-02-18	cc-1	2353 ± 11	30.9 ± 0.3	13.8 ± 0.3	B	
	2011-01-13	cc-1	2339 ± 7	31.5 ± 0.2	14.2 ± 0.4	B	
	2010-02-18	cc-2	2508 ± 11	342.2 ± 0.3	13.9 ± 0.3	B	
	2011-01-13	cc-2	2489 ± 7	342.7 ± 0.2	14.2 ± 0.3	B	
	2010-02-18	cc-3	3152 ± 11	67.6 ± 0.2	12.2 ± 0.1	B	
	2011-01-13	cc-3	3178 ± 7	68.1 ± 0.2	12.8 ± 0.1	B	
	2010-02-18	cc-4	4968 ± 11	94.0 ± 0.2	13.4 ± 0.2	B	
	2011-01-13	cc-4	5003 ± 6	94.1 ± 0.1	14.0 ± 0.3	B	
	2010-02-18	cc-5	5231 ± 12	241.6 ± 0.2	8.9 ± 0.1	B	
	2011-01-13	cc-5	5210 ± 8	241.2 ± 0.1	9.4 ± 0.1	B	
	2010-02-18	cc-6	5355 ± 12	71.1 ± 0.2	11.7 ± 0.1	B	
	2011-01-13	cc-6	5387 ± 7	71.3 ± 0.1	12.4 ± 0.1	B	
	2010-02-18	cc-7	5602 ± 12	24.6 ± 0.1	9.1 ± 0.1	B	
	2011-01-13	cc-7	5599 ± 8	25.0 ± 0.1	9.7 ± 0.1	B	
	2010-02-18	cc-8	5712 ± 12	27.8 ± 0.1	12.7 ± 0.1	B	
	2011-01-13	cc-8	5717 ± 9	28.0 ± 0.1	13.2 ± 0.1	B	
	2010-02-18	cc-9	5801 ± 12	245.6 ± 0.1	10.2 ± 0.1	B	
	2011-01-13	cc-9	5776 ± 8	245.3 ± 0.1	10.7 ± 0.1	B	
	2010-02-18	cc-10	5833 ± 11	102.6 ± 0.2	13.4 ± 0.2	B	
	2011-01-13	cc-10	5879 ± 7	102.6 ± 0.1	14.0 ± 0.2	B	
	2010-02-18	cc-11	6097 ± 12	107.7 ± 0.1	12.6 ± 0.1	B	
	2011-01-13	cc-11	6138 ± 7	107.7 ± 0.1	13.3 ± 0.1	B	
	2010-02-18	cc-12	6951 ± 13	147.5 ± 0.1	13.6 ± 0.2	B	
	2011-01-13	cc-12	6990 ± 10	147.4 ± 0.1	14.4 ± 0.4	B	
	2010-02-18	cc-13	3369 ± 11	165.3 ± 0.2	14.3 ± 0.3	U	
	2010-02-18	cc-14	5948 ± 13	228.5 ± 0.1	15.0 ± 0.4	U	
	2011-01-13	cc-15	7049 ± 7	9.4 ± 0.1	12.9 ± 0.1	U	
TYC 7188-0575-1	2010-02-16	cc-1	4238 ± 15	296.5 ± 0.2	15.2 ± 0.4	B	SB2
	2011-01-27	cc-1	4148 ± 12	297.5 ± 0.2	14.8 ± 0.4	B	
	2010-02-16	cc-2	4741 ± 15	61.7 ± 0.2	11.6 ± 0.1	B	
	2011-01-27	cc-2	4843 ± 12	62.2 ± 0.2	11.4 ± 0.1	B	
	2010-02-16	cc-3	5329 ± 15	186.0 ± 0.2	11.9 ± 0.1	B	
	2011-01-27	cc-3	5303 ± 11	185.1 ± 0.2	11.8 ± 0.1	B	
	2010-02-16	cc-4	7391 ± 15	279.5 ± 0.2	13.2 ± 0.2	B	
	2011-01-27	cc-4	7282 ± 11	279.8 ± 0.1	13.1 ± 0.2	B	
	2010-02-16	cc-5	8020 ± 15	5.1 ± 0.2	11.6 ± 0.1	B	
	2011-01-27	cc-5	8058 ± 11	5.8 ± 0.1	11.7 ± 0.1	B	
TYC 6069-1214-1	2010-02-17	none					
TYC 7722-0207-1	2010-02-17	cc-1	3981 ± 11	33.5 ± 0.2	11.7 ± 0.1	B	
	2011-01-29	cc-1	3978 ± 6	35.0 ± 0.1	11.5 ± 0.1	B	
	2010-02-17	cc-2	4369 ± 12	228.1 ± 0.2	7.3 ± 0.1	B	
	2011-01-29	cc-2	4355 ± 7	226.9 ± 0.1	7.1 ± 0.1	B	
	2010-02-17	cc-3	8516 ± 11	105.2 ± 0.1	9.4 ± 0.1	B	
	2011-01-29	cc-3	8602 ± 6	105.4 ± 0.1	9.1 ± 0.1	B	
	2010-02-17	cc-4	1742 ± 10	329.8 ± 0.3	13.9 ± 0.5	U	
	2011-01-29	cc-5	7958 ± 11	317.3 ± 0.1	10.1 ± 0.1	U	
	2011-01-29	cc-6	7988 ± 11	42.2 ± 0.1	12.4 ± 0.1	U	

Table 9. Companion candidates characterization and identification (for multi-epoch observations). Table 8-cont.

Name-1	UT-Date	Nb Cand.	Sep (mas)	PA (deg)	ΔH (mag)	Status	Comments
TYC 7743-1091-1	2010-02-19	none					
HIP58240	2010-02-16	cc-1	5761 ± 21	179.6 ± 0.2	13.0 ± 0.2	B	
	2011-01-29	cc-1	5770 ± 5	178.1 ± 0.1	12.9 ± 0.1	B	
TYC 9231-1566-1	2010-02-19	none					New binary (see Table 6)
TYC 8979-1683-1	2010-02-18	54(+16)					Electronic table
	2011-05-11	54				B(+U)	Electronic table
TYC 8989-0583-1	2010-02-18	none					New binary (see Table 6)
	2010-06-16	none					
TYC 9245-0617-1	2010-02-18	cc-1	3771 ± 10	32.2 ± 0.2	9.5 ± 0.1	B	
	2013-02-11	cc-1	3860 ± 5	33.2 ± 0.1	9.1 ± 0.1	B	
	2010-02-18	cc-2	3942 ± 10	119.4 ± 0.2	5.9 ± 0.1	B	
	2011-04-04	cc-2	3974 ± 10	118.9 ± 0.2	6.0 ± 0.1	B	
	2013-02-11	cc-2	4015 ± 5	118.4 ± 0.1	5.8 ± 0.1	B	
	2010-02-18	cc-3	6544 ± 9	183.4 ± 0.1	10.9 ± 0.1	B	
	2013-02-11	cc-3	6517 ± 3	182.4 ± 0.1	10.9 ± 0.3	B	
	2010-02-18	cc-4	7448 ± 11	241.0 ± 0.1	10.2 ± 0.1	B	
	2013-02-11	cc-4	7342 ± 8	241.0 ± 0.1	10.2 ± 0.2	B	
	2010-02-18	cc-5	4590 ± 10	306.1 ± 0.1	12.8 ± 0.1	U	
	2010-02-18	cc-6	5603 ± 9	263.3 ± 0.1	14.5 ± 0.3	U	
	2010-02-18	cc-7	5887 ± 9	179.7 ± 0.1	12.2 ± 0.1	U	
	2010-02-18	cc-8	6149 ± 10	251.4 ± 0.1	13.3 ± 0.2	U	
	2010-02-18	cc-9	7432 ± 12	146.0 ± 0.1	11.9 ± 0.1	U	
	2010-02-18	cc-10	8529 ± 10	73.1 ± 0.1	12.9 ± 0.2	U	
HIP63862	2010-02-18	cc-1	4231 ± 16	28.0 ± 0.2	12.9 ± 0.1	B	
	2011-07-02	cc-1	4315 ± 5	30.7 ± 0.1	13.1 ± 0.1	B	
	2010-02-18	cc-2	5536 ± 17	206.7 ± 0.2	12.8 ± 0.1	B	
	2011-07-02	cc-2	5478 ± 5	204.8 ± 0.1	13.3 ± 0.1	B	
	2011-07-02	cc-3	7186 ± 5	160.1 ± 0.1	14.1 ± 0.2	U	
	2011-07-02	cc-4	8169 ± 10	142.8 ± 0.1	12.7 ± 0.1	U	
TYC 7796-2110-1	2010-02-16	cc-1	3264 ± 15	127.0 ± 0.3	11.3 ± 0.1	B	
	2011-05-11	cc-1	3306 ± 4	126.3 ± 0.1	11.1 ± 0.3	B	
	2013-03-22	cc-1	3314 ± 9	125.2 ± 0.2	11.2 ± 0.1	B	
	2010-02-16	cc-2	3990 ± 16	141.6 ± 0.2	8.7 ± 0.1	B	
	2011-05-11	cc-2	4018 ± 5	141.1 ± 0.1	8.8 ± 0.1	B	
	2013-03-22	cc-2	4034 ± 9	140.3 ± 0.1	8.7 ± 0.1	B	
	2010-02-16	cc-3	4111 ± 15	109.7 ± 0.2	13.5 ± 0.2	B	
	2013-03-22	cc-3	4190 ± 8	108.5 ± 0.1	13.6 ± 0.3	B	
	2010-02-16	cc-4	5231 ± 16	151.6 ± 0.2	13.2 ± 0.1	B	
	2013-03-22	cc-4	5194 ± 10	150.7 ± 0.1	13.3 ± 0.2	B	
	2010-02-16	cc-5	6324 ± 17	214.1 ± 0.2	12.5 ± 0.1	B	
	2013-03-22	cc-5	6211 ± 11	214.0 ± 0.1	12.4 ± 0.1	B	
	2010-02-16	cc-6	7111 ± 16	62.6 ± 0.2	10.8 ± 0.1	B	
	2011-05-11	cc-6	7145 ± 7	62.8 ± 0.1	11.1 ± 0.3	B	
	2013-03-22	cc-6	7240 ± 10	62.8 ± 0.1	10.8 ± 0.1	B	
	2010-02-16	cc-7	8743 ± 18	48.5 ± 0.1	14.0 ± 0.4	U	
TYC 9010-1272-1	2010-02-18	none					New binary (see Table 6)
HIP70351	2010-02-17	cc-1	2971 ± 10	258.4 ± 0.2	14.7 ± 0.4	U	
	2010-02-17	cc-2	4664 ± 11	288.7 ± 0.2	11.4 ± 0.1	U	
	2010-02-17	cc-3	4973 ± 10	4.0 ± 0.2	13.9 ± 0.2	U	
	2010-02-17	cc-4	6572 ± 10	262.2 ± 0.1	13.5 ± 0.1	U	
	2010-02-17	cc-5	6615 ± 13	235.8 ± 0.1	13.0 ± 0.1	U	
	2010-02-17	cc-6	6820 ± 13	145.7 ± 0.1	11.0 ± 0.1	U	
	2010-02-17	cc-7	7266 ± 12	118.2 ± 0.1	12.9 ± 0.1	U	
HIP71908	2010-02-16	cc-1	6404 ± 16	28.4 ± 0.2	16.3 ± 0.4	U	
HIP71933	2010-06-15	cc-1	4934 ± 9	12.6 ± 0.1	10.0 ± 0.1	B	
	2011-04-06	cc-1	4952 ± 2	12.8 ± 0.1	9.4 ± 0.1	B	
	2013-02-23	cc-1	5031 ± 3	13.1 ± 0.1	10.0 ± 0.1	B	
	2010-06-15	cc-2	5864 ± 11	54.1 ± 0.1	11.3 ± 0.1	B	
	2013-02-23	cc-2	5958 ± 7	54.0 ± 0.1	11.3 ± 0.1	B	

Table 10. Companion candidates characterization and identification (for multi-epoch observations). Table 9-cont.

Name-1	UT-Date	Nb Cand.	Sep (mas)	PA (deg)	ΔH (mag)	Status	Comments
HIP71933	2010-06-15	cc-3	7987 ± 9	12.5 ± 0.1	10.4 ± 0.1	B	
	2011-04-06	cc-3	8006 ± 3	12.8 ± 0.1	9.8 ± 0.2	B	
	2013-02-23	cc-3	8096 ± 4	13.1 ± 0.1	10.4 ± 0.1	B	
	2010-06-15	cc-4	9258 ± 12	205.1 ± 0.1	9.2 ± 0.1	B	
	2013-02-23	cc-4	9127 ± 8	205.1 ± 0.1	9.5 ± 0.1	B	
	2010-06-15	cc-5	5434 ± 10	22.6 ± 0.1	13.3 ± 0.1	U	
	2010-06-15	cc-6	6963 ± 10	107.8 ± 0.1	13.9 ± 0.2	U	
	2010-06-15	cc-7	7158 ± 12	130.1 ± 0.1	12.4 ± 0.1	U	
	2010-06-15	cc-8	7968 ± 11	202.0 ± 0.1	13.9 ± 0.3	U	
	2010-06-15	cc-9	8756 ± 9	12.5 ± 0.1	12.9 ± 0.2	U	
HIP72399	2011-05-27	none					SB1, RV var
TYC 7835-2569-1	2011-05-11	none					SB2 + Known binary[b]
HIP76829	2010-06-15	cc-1	2393 ± 4	46.8 ± 0.1	15.0 ± 0.4	B	
	2011-06-27	cc-1	2705 ± 9	45.7 ± 0.2	14.5 ± 0.5	B	
	2010-06-15	cc-2	6368 ± 6	111.7 ± 0.1	14.8 ± 0.3	B	
	2011-06-27	cc-2	6434 ± 10	109.1 ± 0.1	14.2 ± 0.3	B	
	2010-06-15	cc-3	4481 ± 6	310.5 ± 0.1	16.3 ± 0.6	U	
	2010-06-15	cc-4	5272 ± 3	272.4 ± 0.1	16.3 ± 0.4	U	
	2010-06-15	cc-5	5900 ± 3	91.3 ± 0.1	16.2 ± 0.4	U	
	2010-06-15	cc-6	8618 ± 11	142.8 ± 0.1	15.2 ± 0.4	U	
TYC 6781-0415-1	2011-07-20	none					
TYC 6786-0811-1	2010-07-29	none					Known binary[c]
HIP78747	2010-07-29	cc-1	3892 ± 2	0.6 ± 0.1	11.9 ± 0.1	B	
	2011-06-28	cc-1	3990 ± 4	2.2 ± 0.1	12.0 ± 0.1	B	
	2010-07-29	cc-2	6154 ± 5	292.2 ± 0.1	12.8 ± 0.1	B	
	2011-06-28	cc-2	6110 ± 6	293.5 ± 0.1	13.0 ± 0.2	B	
	2010-07-29	cc-3	6633 ± 8	53.9 ± 0.1	12.7 ± 0.1	B	
	2011-06-28	cc-3	6788 ± 9	53.9 ± 0.1	12.8 ± 0.2	B	
	2010-07-29	cc-4	5508 ± 6	59.0 ± 0.1	14.6 ± 0.2	U	
	2010-07-29	cc-5	5949 ± 2	1.1 ± 0.1	14.7 ± 0.3	U	
	2010-07-29	cc-6	7557 ± 5	200.8 ± 0.1	14.0 ± 0.2	U	
	2011-06-28	cc-7	7419 ± 5	255.3 ± 0.1	13.2 ± 0.2	U	
TYC 6209-0769-1	2011-08-19	cc-1	5473 ± 3	198.6 ± 0.1	8.2 ± 0.1	U	
HIP79958	2011-06-27	cc-1	3583 ± 4	29.3 ± 0.1	11.7 ± 0.3	U	
	2011-06-27	cc-2	3689 ± 1	88.8 ± 0.1	9.4 ± 0.1	U	
	2011-06-27	cc-3	4120 ± 2	281.1 ± 0.1	10.2 ± 0.1	U	
	2011-06-27	cc-4	4633 ± 4	151.3 ± 0.1	11.5 ± 0.2	U	
	2011-06-27	cc-5	5986 ± 2	169.4 ± 0.1	10.9 ± 0.1	U	
	2011-06-27	cc-6	6195 ± 1	177.4 ± 0.1	10.6 ± 0.1	U	
	2011-06-27	cc-7	7628 ± 2	350.9 ± 0.1	11.3 ± 0.3	U	
HIP80290	2011-08-08	cc-1	2688 ± 1	184.6 ± 0.1	8.5 ± 0.1	B	
	2012-08-12	cc-1	2665 ± 7	184.3 ± 0.2	9.1 ± 0.1	B	
	2011-08-08	cc-2	3340 ± 1	257.5 ± 0.1	1.9 ± 0.1	C	
	2012-08-12	cc-2	3335 ± 8	257.6 ± 0.2	2.6 ± 0.1	C	New binary (see Table 6)
	2011-08-08	cc-3	7425 ± 9	143.6 ± 0.1	6.9 ± 0.1	B	
	2012-08-12	cc-3	7417 ± 12	143.4 ± 0.1	7.6 ± 0.1	B	
	2012-08-12	cc-4	2097 ± 8	34.3 ± 0.2	12.4 ± 0.3	U	
	2012-08-12	cc-5	2245 ± 8	291.3 ± 0.2	11.1 ± 0.1	U	
	2012-08-12	cc-6	6186 ± 8	94.6 ± 0.1	12.0 ± 0.1	U	
	2012-08-12	cc-7	8629 ± 11	298.8 ± 0.1	11.0 ± 0.1	U	
HIP80758	2010-07-29	cc-1	2210 ± 3	163.6 ± 0.1	12.9 ± 0.1	B	
	2011-05-11	cc-1	2171 ± 7	163.3 ± 0.2	12.2 ± 0.2	B	
	2010-07-29	cc-2	2221 ± 4	241.1 ± 0.1	12.5 ± 0.1	B	
	2011-05-11	cc-2	2192 ± 7	242.1 ± 0.2	11.8 ± 0.2	B	
	2010-07-29	cc-3	2413 ± 4	321.1 ± 0.1	12.8 ± 0.1	B	
	2011-05-11	cc-3	2455 ± 7	321.7 ± 0.2	12.3 ± 0.2	B	
	2010-07-29	cc-4	4686 ± 6	236.1 ± 0.1	11.5 ± 0.1	B	
	2011-05-11	cc-4	4651 ± 8	236.6 ± 0.1	10.9 ± 0.1	B	
	2010-07-29	cc-5	5228 ± 7	304.1 ± 0.1	12.7 ± 0.1	B	
	2011-05-11	cc-5	5256 ± 9	304.6 ± 0.1	12.1 ± 0.1	B	
	2010-07-29	cc-6	5229 ± 5	70.3 ± 0.1	13.9 ± 0.2	B	
	2011-05-11	cc-6	5215 ± 8	69.9 ± 0.1	12.9 ± 0.2	B	

(b): Known binary (Brandner et al. 1996)
(c): Known binary (Köhler et al. 2000)

Table 11. Companion candidates characterization and identification (for multi-epoch observations). Table 10-cont.

Name-1	UT-Date	Nb Cand.	Sep (mas)	PA (deg)	ΔH (mag)	Status	Comments
HIP80758	2010-07-29	cc-7	5441 ± 5	108.0 ± 0.1	11.9 ± 0.1	B	
	2011-05-11	cc-7	5418 ± 7	107.7 ± 0.1	10.9 ± 0.1	B	
	2010-07-29	cc-8	5489 ± 6	25.2 ± 0.1	10.2 ± 0.1	B	
	2011-05-11	cc-8	5523 ± 8	24.8 ± 0.1	9.6 ± 0.1	B	
	2010-07-29	cc-9	7495 ± 4	79.1 ± 0.1	6.7 ± 0.1	B	
	2011-05-11	cc-9	7472 ± 7	78.7 ± 0.1	5.7 ± 0.1	B	
	2010-07-29	cc-10	7925 ± 3	265.4 ± 0.1	12.7 ± 0.2	B	
	2011-05-11	cc-10	7897 ± 7	265.5 ± 0.1	12.4 ± 0.3	B	
	2010-07-29	cc-11	3005 ± 4	22.0 ± 0.1	14.4 ± 0.3	U	
TYC 6818-1336-1	2011-07-20	cc-1	3382 ± 10	302.7 ± 0.2	7.3 ± 0.1	U	
	2011-07-20	cc-2	5824 ± 10	291.7 ± 0.1	5.5 ± 0.1	U	
	2011-07-20	cc-3	8914 ± 14	52.1 ± 0.1	2.8 ± 0.1	U	
TYC 6815-0084-1	2013-06-02	none					SB2?
TYC 6815-0874-1	2012-08-13	cc-1	2094 ± 16	229.6 ± 0.4	12.2 ± 0.2	U	
	2012-08-13	cc-2	2224 ± 16	333.4 ± 0.4	11.9 ± 0.2	U	
	2012-08-13	cc-3	2713 ± 16	280.7 ± 0.4	12.8 ± 0.2	U	
	2012-08-13	cc-4	2754 ± 16	12.8 ± 0.3	11.1 ± 0.1	U	
	2012-08-13	cc-5	3801 ± 16	171.0 ± 0.3	9.6 ± 0.1	U	
	2012-08-13	cc-6	4035 ± 17	36.9 ± 0.2	12.1 ± 0.1	U	
	2012-08-13	cc-7	4940 ± 17	164.2 ± 0.2	13.2 ± 0.2	U	
	2012-08-13	cc-8	6046 ± 17	285.5 ± 0.2	12.9 ± 0.2	U	
	2012-08-13	cc-9	6569 ± 17	22.6 ± 0.2	13.1 ± 0.2	U	
	2012-08-13	cc-10	8354 ± 19	306.1 ± 0.1	12.4 ± 0.2	U	
	2012-08-13	cc-11	9053 ± 19	125.0 ± 0.1	12.0 ± 0.1	U	
TYC 7362-0724-1	2010-06-16	57(+211)					Electronic table
	2011-05-11	57				B(+U)	Electronic table
TYC 8728-2262-1	2011-08-25	cc-1	2821 ± 12	254.8 ± 0.3	9.1 ± 0.1	U	
	2011-08-25	cc-2	4449 ± 13	27.5 ± 0.2	11.4 ± 0.1	U	
	2011-08-25	cc-3	6232 ± 14	130.2 ± 0.1	12.1 ± 0.2	U	
	2011-08-25	cc-4	6399 ± 12	99.3 ± 0.2	6.3 ± 0.0	U	
	2011-08-25	cc-5	6883 ± 12	166.3 ± 0.1	12.4 ± 0.1	U	
HIP86672	2010-06-16	261					Electronic table
	2011-08-25	none					
	2013-04-25	80(+181)				B(+U)	Electronic table
HIP89829	2011-06-13	99					Electronic table
	2012-08-09	29(+70)				B(+U)	Electronic table
HIP93375	2010-06-14	cc-1	3208 ± 11	121.6 ± 0.2	13.8 ± 0.2	B	
	2011-05-30	cc-1	3175 ± 9	120.5 ± 0.2	13.6 ± 0.2	B	
	2010-06-14	cc-2	4261 ± 10	9.2 ± 0.2	13.7 ± 0.2	B	
	2011-05-30	cc-2	4335 ± 8	9.0 ± 0.2	13.4 ± 0.2	B	
	2010-06-14	cc-3	4595 ± 10	264.5 ± 0.2	12.5 ± 0.1	B	
	2011-05-30	cc-3	4591 ± 8	265.7 ± 0.2	12.8 ± 0.1	B	
	2010-06-14	cc-4	4822 ± 12	139.6 ± 0.1	11.4 ± 0.1	B	
	2011-05-30	cc-4	4754 ± 10	138.9 ± 0.1	11.5 ± 0.1	B	
	2010-06-14	cc-5	5308 ± 10	173.7 ± 0.2	13.7 ± 0.2	B	
	2011-05-30	cc-5	5218 ± 8	173.6 ± 0.1	13.5 ± 0.1	B	
	2010-06-14	cc-6	5354 ± 10	176.9 ± 0.2	14.0 ± 0.2	B	
	2011-05-30	cc-6	5283 ± 8	177.1 ± 0.1	14.0 ± 0.2	B	
	2010-06-14	cc-7	6095 ± 10	274.5 ± 0.1	12.0 ± 0.1	B	
	2011-05-30	cc-7	6104 ± 8	275.2 ± 0.1	12.7 ± 0.1	B	
	2010-06-14	cc-8	6848 ± 10	185.1 ± 0.1	12.4 ± 0.1	B	
	2011-05-30	cc-8	6763 ± 8	184.9 ± 0.1	11.6 ± 0.1	B	
	2010-06-14	cc-9	6942 ± 12	153.9 ± 0.1	12.4 ± 0.1	B	
	2011-05-30	cc-9	6856 ± 10	154.2 ± 0.1	11.6 ± 0.1	B	
	2010-06-14	cc-10	7089 ± 14	46.6 ± 0.1	12.9 ± 0.1	B	
	2011-05-30	cc-10	7143 ± 12	45.8 ± 0.1	13.5 ± 0.2	B	
	2010-06-14	cc-11	7502 ± 13	116.6 ± 0.1	11.1 ± 0.1	U	
	2010-06-14	cc-12	7512 ± 12	115.1 ± 0.1	12.6 ± 0.1	U	
	2011-05-30	cc-13	4157 ± 9	237.0 ± 0.1	14.1 ± 0.2	U	
	2011-05-30	cc-14	5917 ± 8	262.2 ± 0.1	14.4 ± 0.3	U	
	2011-05-30	cc-15	9234 ± 14	322.3 ± 0.1	11.5 ± 0.1	U	

Table 12. Companion candidates characterization and identification (for multi-epoch observations). Table 11-cont.

Name-1	UT-Date	Nb Cand.	Sep (mas)	PA (deg)	ΔH (mag)	Status	Comments
HIP94235	2010-07-30	none					New binary (see Table 6)
TYC 6893-1391-1	2011-06-08	cc-1	3289 ± 4	229.6 ± 0.1	11.2 ± 0.2	U	
	2011-06-08	cc-2	3373 ± 1	256.6 ± 0.1	11.8 ± 0.3	U	
	2011-06-08	cc-3	5761 ± 7	224.5 ± 0.1	6.8 ± 0.0	U	
TYC 5206-0915-1	2010-07-30	none					
TYC 5736-0649-1	2011-08-18	cc-1	4360 ± 6	206.3 ± 0.1	9.8 ± 0.1	U	
	2011-08-18	cc-2	6130 ± 8	306.9 ± 0.1	10.6 ± 0.1	U	
HD189285	2011-08-20	cc-1	4519 ± 4	24.9 ± 0.1	9.5 ± 0.1	U	
HIP98470	2010-06-15	none					
TYC 5164-567-1	2011-07-29	cc-1	2632 ± 3	207.5 ± 0.1	3.3 ± 0.0	U	
	2011-07-29	cc-2	4421 ± 5	56.8 ± 0.1	11.2 ± 0.1	U	
	2011-07-29	cc-3	5674 ± 7	229.3 ± 0.1	8.6 ± 0.1	U	
	2011-07-29	cc-4	7254 ± 9	139.8 ± 0.1	9.8 ± 0.1	U	
HIP99273	2010-07-31	none					
HD199058	2010-06-15	none					New binary (see Table 6)
HIP105384	2010-07-31	none					
	2011-06-08	cc-1	7038 ± 7	24.5 ± 0.1	14.1 ± 0.2	U	
HIP105612	2010-07-31	none					
HIP107684	2010-06-15	none					New binary (see Table 6)
HIP108422	2010-07-30	none					Known binary[d]
TYC 8004-0083-1	2010-06-15	none					
HIP114046	2010-06-15	none					
TYC 9338-2016-1	2009-11-23	none					
	2010-07-30	none					
TYC 9529-0340-1	2010-07-31	none					
TYC 9339-2158-1	2010-07-31	none					
TYC 6406-0180-1	2010-07-30	none					
HIP116910	2009-11-22	none					

(d): Known binary (Chauvin et al. 2010)